The Role of Nuclear Factor Kappa B

in Myeloid Cells During Lung Carcinogenesis

By

Allyson Perry

Dissertation

Submitted to the Faculty of the

Graduate School of Vanderbilt University

in partial fulfillment of the requirements

for the degree of

DOCTOR OF PHILOSOPHY

in

Cancer Biology

December 2016

Nashville, Tennessee

Approved:

Timothy Blackwell, M.D.

Barbara Fingleton, Ph.D.

Ann Richmond, Ph.D.

Pampee Young, M.D., Ph.D.

To my parents, Larry and Debbie McLoed, for their unwavering support

To my teachers for fostering in me a pursuit for knowledge and excellence

And to my loving husband, Jacob Perry, for always believing in me

ACKNOWLEDGMENTS

The completion of this milestone in my life would not have been possible without the support, encouragement, instruction, and feedback from my mentor, committee members, lab mates, family, and friends. Any success that I have had at Vanderbilt is attributed to them, and I hope that I have made them proud.

First and foremost, I thank my mentor, Tim Blackwell, for making a home for me in his laboratory and for supporting me financially, educationally, and personally. Even as a division director, physician, and leader of a sizeable lab that studies multiple lung diseases, he still managed to stay up-to-speed on the developments of my project and most of the time even knew what I was talking about when I said vague things like, "I ran that western..." One of the most significant things I learned from Tim was to see the forest before focusing on the trees. He taught me not to limit my ideas to the tools at hand but to instead design a project that answered important biological questions and had implications for patient care. Tim pushed me to be an independent thinker and self-sufficient scientist, two important attributes that will serve me well in the future. I am especially thankful to Tim for being supportive of my decision to step away from the bench and move into an "alternate" career of medical writing, which is something I truly enjoy doing. Finally, I cannot thank him enough for being such a wonderful boss and for making my time at Vanderbilt such a rewarding experience.

I would also like to thank the other members of my thesis committee, Barbara Fingleton, Ann Richmond, and Pampee Young for keeping me on my toes and being intimidating enough that I was always prepared for meetings! Each member of the committee brought a unique perspective to our meetings and was instrumental in helping me shape my project and package it into a publication. I thank Barbara first for her contribution to my education as a teacher in the Cancer Biology department, second for

her willingness to serve as my committee chair, and third for her genuine interest in my life and my work. I thank Ann for all of her critiques, suggestions, and career advice. I think I learned something new about NF-κB from her every meeting. Ann was also kind enough to lend me reagents and have her lab members teach me new techniques. Finally, I thank Pampee for willingness to serve on a committee outside of her own department. Her clinical perspective as well as expertise in myeloid cells was most helpful as I designed experiments and considered the clinical significance of my work. Pampee also connected me with a colleague of hers to learn about handling neutrophils *ex vivo*, a technique that was crucial for my studies. I thank all of my committee members for taking time out of their busy schedules to advise me during my training.

The members of the Blackwell lab, past and present, have been true champions throughout my graduate career, and I could not have completed my training without them. Thanks goes first to Rinat Zaynagetdinov, who was a second mentor to me and who helped my project get up and running. I cannot thank him enough for his guidance, technical training, career advice, and friendship. Rinat taught me how to tell a scientific story and how to package my data into a straightforward manuscript even though we all know that the road had a lot of twists and turns along the way. I can't imagine my graduate career without him. Another person who was with me every step of the way was my fellow graduate student, Jamie Saxon. I thank Jamie for her friendship and for setting an impressive example of hard work, perseverance, talent, and intellect. The members of the Blackwell lab taught me everything I know about mouse surgery and basic science analyses, but even more, they became good friends that will not be forgotten. Thank you to Ankita Burman, Harikrishna Tanjore, Pierre Hunt, Taylor Sherrill, Wei Han, Dong-sheng Cheng, Jonathan Kropski, Linda Gleaves, Bradley Richmond, and Vasiliy Polosukhin for their encouragement, patience, and support.

Outside of the academic setting, I am so thankful to my family and friends for encouraging me and listening to me ramble even if they had no idea what I was talking about. I could not ask for better parents. They taught me the value of a good education and made it possible for me to come this far. Whenever I would ask my dad a question, he would say "look it up!" Little did he know that "looking it up" is what I will spend the remainder of my career doing! Beyond education, they taught me to maintain perspective and not to sweat the small stuff (or even most of the "big" stuff). My mom always taught me to do my best and that my best was all I could give. I have returned to that lesson time and time again throughout graduate school. I give a big thank you to my sister for being another science nerd in the family who actually knew what I meant when I said "centrifuge." I'm proud of my little sister for what she has accomplished.

My husband joined me in the middle of my academic journey at Vanderbilt and has never stopped believing that I could finish strong. I am so thankful that God brought him into my life to be a constant source of love, kindness, and encouragement. He has been my biggest cheerleader through these final two years, and without him the journey would have been much more difficult.

Finally, and certainly most importantly, I thank the Lord above for giving me the intellect, strength, opportunity, and perseverance to finish this small race in my life.

TABLE OF CONTENTS

LIST OF TABLES

LIST OF FIGURES

ABBREVIATIONS

AAH   Atypical adenomatous hyperplasia

Adeno   Adenovirus

AIM2   Absent in melanoma 2

ALK   Anaplastic lymphoma kinase

ASC   Apoptosis-associated speck-like protein containing a caspase-recruitment
             domain (CARD)

BAL   Bronchoalveolar lavage

BAY   BAY 11-7082, inhibitor of IκBα phosphorylation

BMT   Bone-marrow transplant

Bort   Bortezomib

Casp1   Caspase-1

CatG   Cathepsin G

CCSP   Clara cell secretory protein

CFSE   Carboxyfluorescein succinimidyl ester fluorescent dye

Cre   Cre recombinase

DAPI   4′,6-diamidino-2-phenylindole blue-fluorescent DNA stain

Dox   Doxycycline

EGFR   Epidermal growth factor receptor

ELISA   Enzyme-linked immunosorbent assay

FACS   Fluorescence-activated cell sorting

FDA   Federal Drug Administration

GLP   Z-GLP-CMK; inhibitor of cathepsin G

H&E   Hematoxylin and eosin stain

IKKβ   Inhibitor of nuclear factor kappa B kinase subunit beta

IL-1β   Interleukin-1 beta

IL-1ra   Interleukin-1 receptor antagonist

IP   Intraperitoneal

IT   Intratracheal

IκB	Inhibitor of κB
KC	Keratinocyte chemoattractant
KO	Knockout
Kras	Kirsten rat sarcoma viral oncogene homolog
LLC	Lewis lung carcinoma cell line
LPS	Lipopolysaccharide
LysM	Lysozyme M
MDSC	Myeloid derived suppressor cell
MeO	MeOSuc-APPV-CMK; inhibitor of neutrophil elastase and proteinase-3
MLR	Multi-leukocyte reaction assay
MMP	Matrix metalloproteinase
MPO	Myeloperoxidase
Mye	Myeloid
NF-κB	Nuclear factor kappa B
NLRP3	Nucleotide-binding domain, leucine-rich repeat (NLR) family, pyrin domain containing 3
NOS	Not otherwise specified (NSCLC histological subtype)
NSCLC	Non-small cell lung cancer
PBS	Phosphate buffered saline
PCNA	Proliferating cell nuclear antigen
PFU	Plaque-forming unit
RT-PCR	Real-time polymerase chain reaction
SCLC	Small cell lung cancer
SPF	Specific pathogen-free
TAM	Tumor-associated macrophage
TAN	Tumor-associated neutrophil
TKI	Tyrosine kinase inhibitor
VEGF	Vascular endothelial growth factor
WT	Wild-type
YVAD	Ac-YVAD-CMK; inhibitor of caspase-1

CHAPTER I: INTRODUCTION

Overview of lung cancer

Risk and survival

In the next several years, cancer is expected to surpass heart disease as the leading cause of death in the United States. Lung cancer has been the foremost cause of cancer-related deaths since the late 1950s for males and since the late 1980s for females. In 2015, it was responsible for more than a quarter of all deaths from cancer (1). The greatest risk factor for lung cancer, as well as the most preventable, is cigarette smoking (2). While reduction in smoking prevalence has reduced lung cancer incidence rates in recent years (3), cigarette smoking still accounts for 87% of lung cancer deaths (2). Lesser contributors to lung cancer incidence include exposure to radon gas, secondhand smoke, asbestos, arsenic, chromium, and nickel. Genetic factors also influence lung cancer susceptibility (4). Despite strong advances in lung cancer screening and treatment strategies, those diagnosed with lung cancer are usually diagnosed with late-stage disease and face a five-year survival rate of only 17% (3).

Histological subclasses

Lung cancer is divided into two major subclasses, small cell lung cancer (SCLC) and non-small cell lung cancer (NSCLC). About 10-15% of lung cancers are SCLCs. SCLC is characterized by tumor cells of small size, a round-to-spindle shape, very little cytoplasm, finely granular nuclear chromatin, and absent or inconspicuous nucleoli. The cells are usually arranged in sheets (**Figure 1A**) (5). NSCLC comprises 85-90% of lung cancers and is further divided into three subgroups, adenocarcinoma, squamous cell

carcinoma, and large cell carcinoma, based on the cells from which it arises. About 40%

of NSCLCs are adenocarcinomas, which arise from the peripheral bronchi (6). Tumor

cells of adenocarcinomas are typically arranged in clusters with sharply defined borders.

The cells have abundant cytoplasm and round to oval nuclei with prominent nucleoli

(**Figure 1B**) (5). Squamous cell carcinomas make up 25-30% of all NSCLCs and arise

from the main bronchi (7). Tumor cells grow in aggregates within flat sheets and may be

spindle- and tadpole-shaped with spindle nuclei. Keritanized cytoplasm is detectable in

well-differentiated tumors (**Figure 1C**) (5). Large cell carcinomas, often also termed

NSCLC "not otherwise specified", make up about 10% of NSCLCs. These tumors lack

the cytologic features of other lung cancer types, are usually proximal, and rapidly

spread locally to the mediastinum (**Figure 1D**) (5, 7).
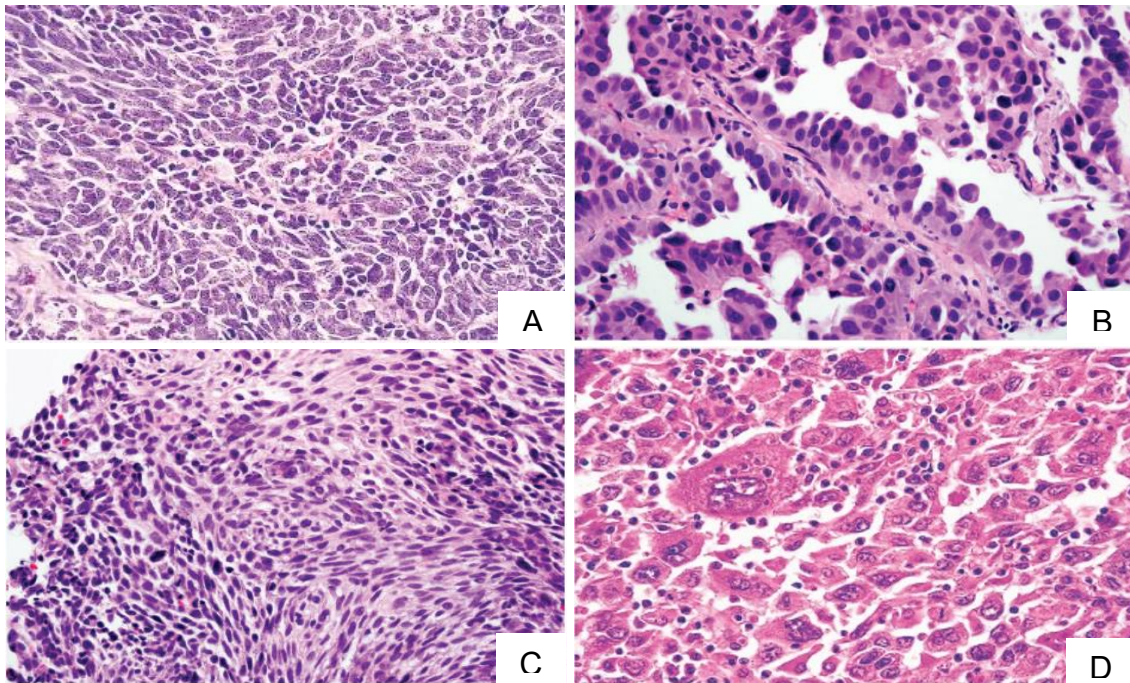
Figure 1: Histopathology of lung cancer subtypes
Tumor biopsy sections stained with H&E. (A) SCLC; (B) Adenocarcinoma; (C) Squamous cell carcinoma; (D) Large cell carcinoma.
(A) and (D) modified and used with permission from Noguchi M, Shimosato Y. (8). Copyright © 2010 Lippincott Williams & Wilkins, a Wolters Kluwer business.
(B) and (C) modified from Travis et al. (9). Originally published by the American Society of Clinical Oncology. Travis WD, Brambilla E, Riely GJ: 8(3), 2013: 992-1001. Used with permission.

Molecular classification of NSCLC

Significant progress in understanding the molecular biology of NSCLC has been made in recent years. Research has identified a number of driver mutations that confer growth advantages to cancer cells and positively select these cells for survival in the lung tumor microenvironment (10). Because these mutations drive oncogenesis, they are prime candidates for pharmacological targeting and have been used to molecularly classify NSCLC. As depicted in **Figure 2**, the most common genetic aberrations in NSCLC adenocarcinomas are activating mutations in Kirsten rat sarcoma viral oncogene homolog (KRAS) and epidermal growth factor receptor (EGFR), which together comprise 40-50% of all NSCLCs. Genetic rearrangement of anaplastic lymphoma kinase (ALK) occurs in 7% of NSCLCs and results in the oncogenic fusion protein echinoderm microtubule-associated protein-like 4 (EML4)-ALK. Other less common mutations include mesenchymal epithelial transition factor (MET), human epidermal growth factor receptor 2 (HER2)/mitogen-activated protein kinase kinase (MEK), B-Raf proto-oncogene (BRAF), ROS Proto-Oncogene 1 (ROS), and ret proto-oncogene (RET) (11). Remarkably, these genetic aberrations tend to be mutually exclusive (12). Driver mutations for squamous cell carcinoma include phosphatidylinositol-4,5-bisphosphate 3-kinase, catalytic subunit alpha (PIK3CA), fibroblast growth factor receptor 1 (FGFR1), MET, discoidin domain receptor tyrosine kinase 2 (DDR2), and BRAF. While therapies have been developed to target some of these mutations, 40% of adenocarcinomas and 33% of squamous cell carcinomas still do not have known driver mutations (11).
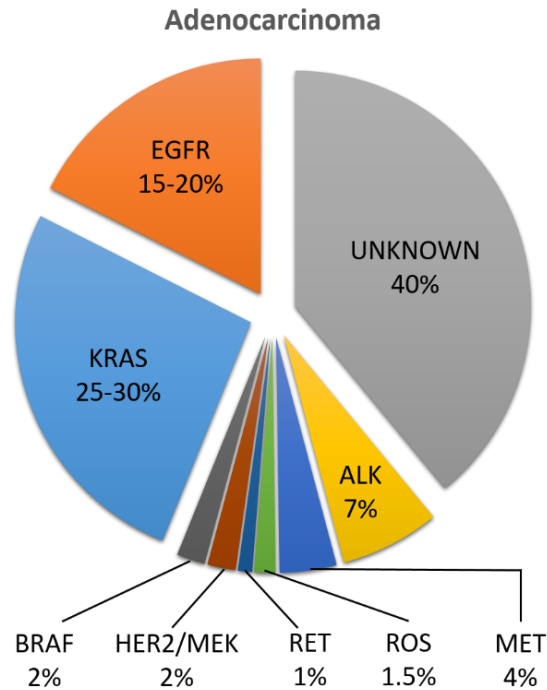
Figure 2: Driver mutations of NSCLC adenocarcinomas
Pie chart showing percentages of NSCLC adenocarcinomas that have specific driver mutations. Modified from Boolel et al. (11). Used with permission under the terms and conditions of the Creative Commons Attribution license (http://creativecommons.org/licenses/by/4.0/).
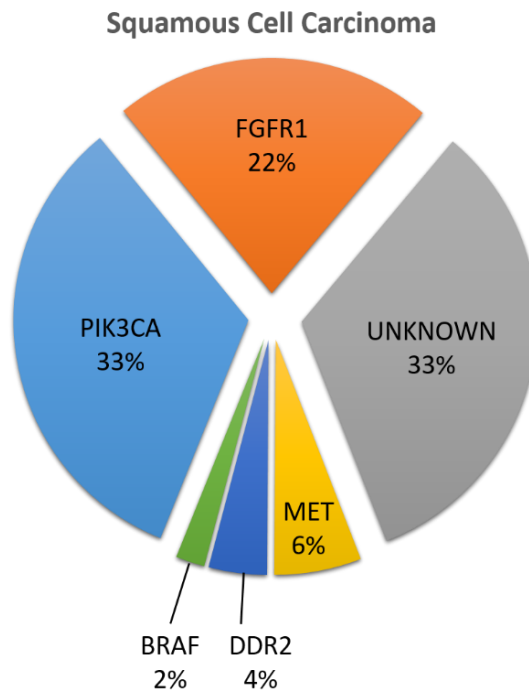
Figure 3: Driver mutations of NSCLC squamous cell carcinoma
Pie chart showing percentages of NSCLC squamous cell carcinomas that have specific driver mutations. Modified from Boolel et al. (11). Used with permission under the terms and conditions of the Creative Commons Attribution license (http://creativecommons.org/licenses/by/4.0/).

Treatment of NSCLC

Treatment of lung cancer is based on tumor histology, grade, and molecular characteristics. Resectable, early-stage NSCLC is usually treated with surgery, which may be followed by chemotherapy with or without radiation (3). Following surgical resection, the five-year survival rate for stage I and II NSCLC patients is 60-80% and 30-50%, respectively (13). While surgery is the best option for prolonging survival in early-stage NSCLC patients (14), the majority of NSCLC patients (over 70%) are diagnosed with non-resectable, advanced-stage disease (9). Treatment for these patients include chemotherapy, targeted therapy, or a combination of the two (3).

With the identification of genetic aberrations in NSCLC, several small molecule inhibitors have been developed to target driver mutations. Gefitinib, erlotinib, and afatinib are tyrosine kinase inhibitors (TKIs) that have been approved by the Federal Drug Administration (FDA) for first-line treatment of advanced or metastatic NSCLC with EGFR mutations (15). Gefitinib and erlotinib are first generation reversible TKIs specifically targeted to the tyrosine kinase domain of EGFR to prevent anti-apoptotic and proliferative signaling (16). They are effective in patients whose tumors have a deletion in exon 19 or an L858R point mutation in exon 21 of EGFR (17–21). However, patients treated with gefitinib or erlotinib develop resistance to therapy within 8-16 months of treatment (22). About half of these patients become resistant through the acquisition of an additional T790M mutation in the tyrosine kinase domain of EGFR (22–24). Afatinib and osimertinib are second generation TKIs that irreversibly bind EGFR and inhibit aberrant signaling resulting from both exon 19 deletions and L858R mutations as well as T790M mutations. Gefitinib- and erlotinib-resistant tumors are sensitive to both afatinib and osimertinib (25–29); however, tumors still develop resistance within months (25, 26, 29).

TKIs crizotinib, ceritinib, and alectinib have been approved by the FDA for treatment of locally advanced or metastatic NSCLCs with ALK gene rearrangements (15). Crizotinib, which inhibits ALK, ROS1, and some MET tyrosine kinases, is more effective both as first-line and subsequent therapy than chemotherapy in patients with ALK-mutant NSCLC (30, 31). However, resistance occurs after about 10 months (32, 33). Ceritinib and alectinib are approved for treatment of crizotinib-resistant NSCLCs with ALK rearrangements. Ceritinib inhibits ALK and insulin-like growth factor 1 (IGF-1), while alectinib inhibits ALK and RET (15). Both drugs have a response rate of about 50% with disease progression occurring 7-12 months after treatment (34, 35).

Since the majority of NSCLCs diagnosed do not harbor EGFR mutations or ALK gene rearrangements, therapies have been developed to inhibit broader targets, including angiogenesis and immune checkpoint proteins (16). Angiogenesis is the formation of new blood vessels, a process that is crucial for sustained tumor growth (36). Bevacizumab is a monoclonal antibody that inhibits angiogenesis by binding to vascular endothelial growth factor A (VEGFA). It has been shown to delay disease progression in combination with chemotherapy and is approved for treatment of advanced non-squamous NSCLC (16, 37–39). The TKI nintedanib inhibits several angiogenesis pathways and, in combination with chemotherapy, has shown particular benefit in patients with adenocarcinoma (16, 40). Nintedanib is approved for treatment of advanced adenocarcinoma after failure of first-line chemotherapy in Europe but has not yet received approval in the United States (16). Unfortunately, benefits from angiogenesis inhibitors, like cancer cell-targeted therapies, last only months before rapid resistance develops (41).

Immune checkpoints are inhibitory pathways within immune cells that are crucial for maintaining self-tolerance and preventing inappropriate immune responses that could be detrimental to the host (16, 42). In lung and other cancers, tumor cells use immune

checkpoints, such as the programmed cell death protein 1 (PD-1) pathway, to render

immune cells tolerant of tumor antigens, thereby evading attack. Tumor cells

overexpress programmed cell death ligands 1 and 2 (PD-L1 and 2), which bind to PD-1

protein on activated T-cells and deactivate them (**Figure 4**) (16). To prevent this

mechanism of immune evasion, immune checkpoint inhibitors, including PD-1 inhibitors,

have been utilized to promote T cell immunity against cancer cells (43–45).

Pembrolizumab is a PD-1 inhibitor approved for treatment of both non-squamous and

squamous NSCLC and is especially effective for tumors with high expression of

programmed cell death ligand 1 (PD-L1) (46). Nivolumab is another FDA-approved PD-1

inhibitor that improves response duration compared to docetaxel in both non-squamous

and squamous NSCLCs (47, 48). Recently, a clinical trial investigating nivolumab

monotherapy vs chemotherapy in patients with previously untreated advanced NSCLC

whose tumors expressed PD-L1 ≥5% (CheckMate-026, NCT02041533) did not meet its

primary endpoint of progression-free survival (49). While the patient population was

broad, these negative results suggest that checkpoint inhibitors may not be quite as

effective as initially believed.
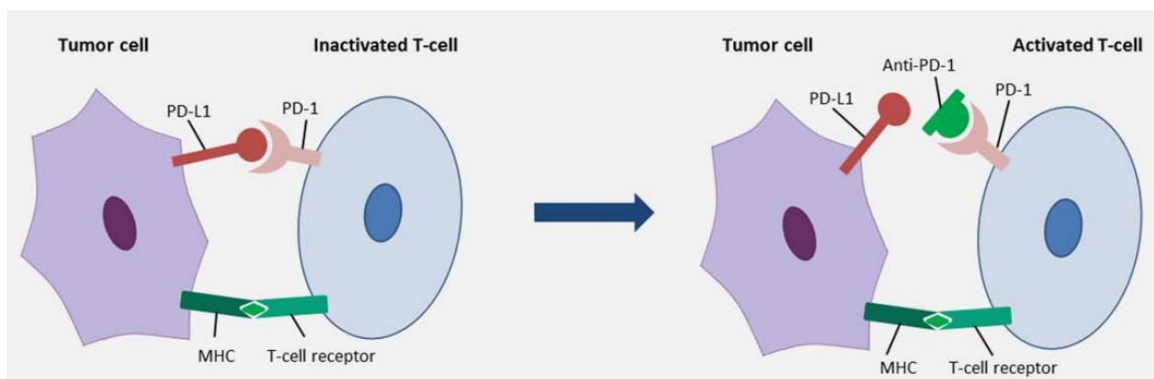
Figure 4: Activation of T cells by anti-PD-1 checkpoint inhibitors
Left: PD-L1 expressed on a tumor cells binds to PD-1 protein on the surface of a T cell and
inactivates the T cell; Right: An anti-PD-1 inhibitor binds to PD-1 protein on the surface of a T cell
and maintains T cell activation. Modified from Minguet et al. (16). Copyright © 1999-2016 John
Wiley & Sons, Inc. All Rights Reserved. Used with permission.

While great strides have been made in NSCLC treatment within the past decade, numerous challenges remain and stress the need for continued development of novel therapeutic strategies. Ultimately, to improve lung cancer survival rates, disease will need to be detected at earlier stages (50). Lung cancer screening for high-risk individuals is imperative to identify candidates for early detection when treatment is likely to be most beneficial. In 2011, the National Lung Screening Trial research team determined that low-dose computed tomography (CT) detected more early-stage NSCLC than radiography and reduced lung cancer mortality (51). Additionally, known and novel driver mutations will need to be effectively targeted. For example, KRAS mutations are present in 15-20% of NSCLC adenocarcinomas, but despite great efforts, no therapy has been established that effectively target mutant KRAS (52).

A large obstacle in NSCLC treatment is the inevitable development of resistance in patients with initial responses. Targeted therapies for EGFR mutations and ALK rearrangements clearly demonstrate the ability of initially sensitive tumors to adapt and exploit various mechanisms to render treatment ineffective. The challenge of treating these patients is to quickly identify and target resistance mechanisms with new drugs to keep the cancer in remission (50). Discovering these resistance mechanisms to treatment is complex and has its own collection of challenges. Lung tumors are a heterogeneous mixture of cancer cells that do not all share the same mutations or respond equally to the same drug. A targeted therapy may eliminate only a subpopulation of the tumor while the remaining cells continue to grow. Additionally, not all tumors employ the same resistance mechanism to specific treatments (50). For example, only 50% of NSCLC tumors with exon 19 deletions or L858R mutations in exon

21 develop targetable T790M mutations (22–24). Patients with other resistance mechanisms have fewer options for subsequent treatment.

The introduction of angiogenesis and checkpoint inhibitors provided NSCLC treatment strategies for patients whose tumors had unknown driver mutations or were resistant to EGFR or ALK inhibitors (16). While these treatments may be beneficial in patients for a time, eventual disease progression is considered inevitable (41, 53). In order to sustain NSCLC remission, a battery of therapies will be required that use different mechanisms to overcome resistance and curb disease progression.

Cancer-related inflammation is one of the hallmarks of cancer and represents target for cancer therapeutics that has not been appreciated until recently. It is characterized by infiltration of the tumor microenvironment by immune cells, increased expression of cytokines and chemokines, tissue remodeling, and angiogenesis (54). Most previous efforts have focused on eliminating tumor cells themselves. However, targeting inflammatory signaling pathways that are critical for maintaining cancer-related inflammation may prove beneficial in single-agent or combination therapy strategies for treating lung and other cancers.

<div align="center">Nuclear factor kappa B</div>

Classical and alternative signaling pathways

Nuclear factor kappa B (NF-κB) is a transcription factor family that regulates expression of over 450 genes involved in numerous cellular processes (55). The five members of the NF-κB family (p65 [RelA], RelB, c-Rel, p105/p50 [NF-κB1], and p100/52 [NF-κB2]) associate with each other to form homodimers or heterodimers that have distinct DNA-binding specificities to κB sites as well as different activation mechanisms

(56). In unstimulated cells, NF-κB dimers are bound to inhibitory proteins and sequestered in the cytoplasm. The NF-κB pathway is activated by a variety of stimuli, including pro-inflammatory cytokines, T- and B-cell mitogens, bacteria, lipopolysaccharide (LPS), viruses, viral proteins, double-stranded RNA, and physical and chemical stresses (57). Upon pathway activation, the inhibitory proteins are phosphorylated and undergo proteasomal degradation, allowing the NF-κB dimers to translocate into the nucleus and control gene transcription (58).

Two distinct NF-κB signaling pathways have been described: the classical (canonical) pathway and the alternative (noncanonical) pathway (**Figure 5**). In the classical pathway, the inhibitor of κB (IκB) becomes phosphorylated by IκB kinase subunit β (IKKβ), resulting in ubiquitination and proteasomal degradation of IκB. The p50/RelA NF-κB heterodimer then translocates to the nucleus and regulates gene transcription. p50/RelA is the prototypical NF-κB heterodimer and is expressed in nearly all cell types. Its activation induces production of mediators involved in immunity, inflammation, proliferation, and apoptosis (58). In the alternative pathway, IKKα phosphorylates the IκB-like C-terminal domain of p100, resulting in proteasomal processing of p100 to p52. The p52/RelB heterodimer then translocates into the nucleus and transcribes downstream target genes (58). While classical NF-κB signaling has been studied extensively, much less is known about the functions of the alternative pathway. However, the alternative NF-κB pathway has been described to play roles in secondary lymphoid organogenesis and architecture organization, thymic epithelial cell differentiation, B-cell maturation and survival, dendritic cell maturation, and bone metabolism (59).
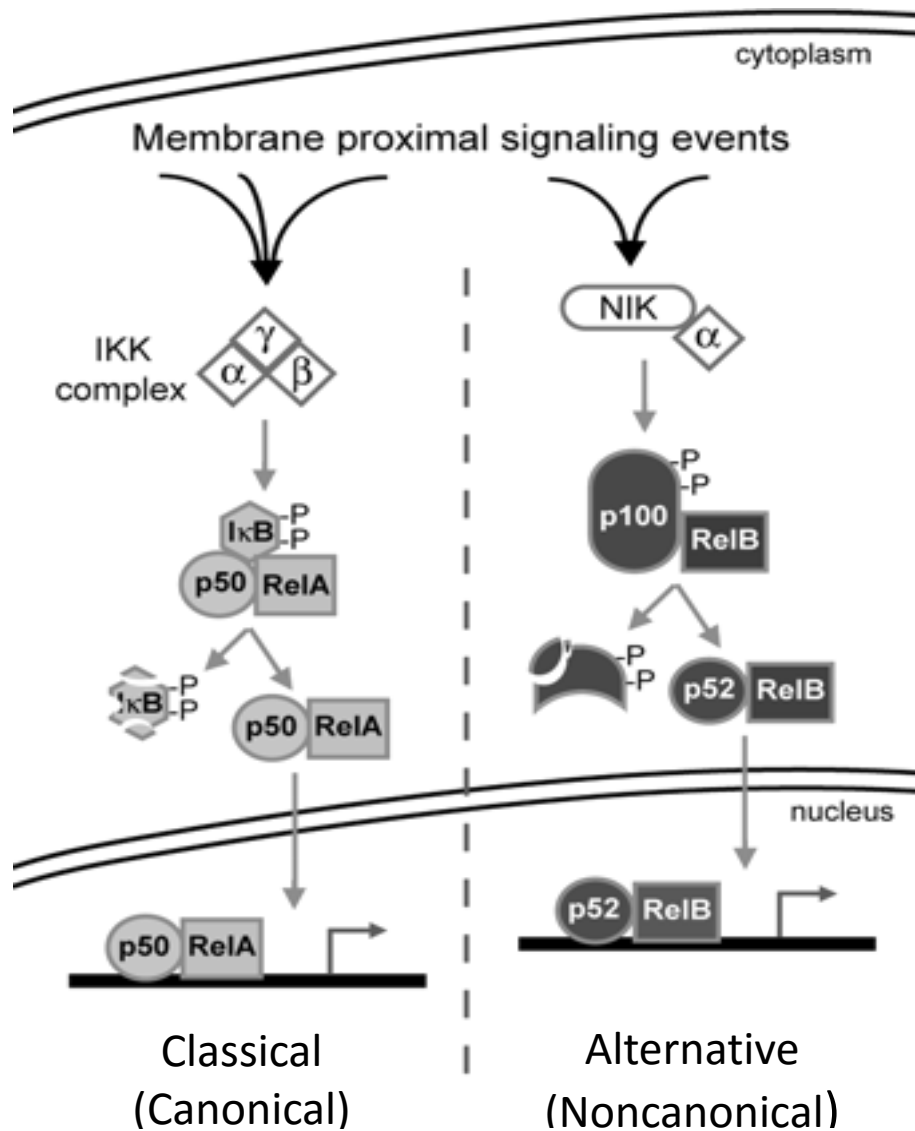
Figure 5: Classical and alternative NF-κB signaling pathways
Left: In the classical pathway, IKKβ phosphorylates IκB, targeting IκB for ubiquitination and subsequent proteasomal degradation. The RelA/p50 heterodimers then translocate to the nucleus and regulated gene transcription. Right: In the alternative pathway, IKKα phosphorylates p100, leading to proteasomal processing of p100 to p52. The p52/RelB heterodimer then translocates to the nucleus and transcribes target genes. Modified and used with permission from Martinka et al. (56). Copyright © 2006 the American Physiological Society.

Most solid and lymphoid tumors have activated NF-κB signaling, though the causes of increased signaling appear to be different. In several B cell malignancies, upstream signaling mediators are mutated or stabilized, resulting in constitutive NF-κB signaling (59–66). However, most solid tumors have enhanced NF-κB activation that is not associated with genetic alterations in NF-κB, IKK, or upstream components within the signaling system. NF-κB activation in lung cancer is significantly associated with increased tumor staging and poor prognosis, but direct mutations in NF-κB pathway proteins have not been observed (67–69). Instead, constitutive NF-κB activation in lung cancer is mediated by activating mutations in oncogenes (EGFR, HER2, BRAF, KRAS, etc.) that crosstalk with NF-κB or inactivating mutations in tumor suppressor genes (P53, RB, PTEN, STK11) that increase NF-κB transcriptional activity (70–74). NF-κB can also be activated by cigarette smoke carcinogens and cigarette smoke-induced chronic lung inflammation (75, 76).

Aberrant NF-κB signaling is recognized as a critical link between inflammation and cancer (77). Several different inflammation-associated cancer models have demonstrated that NF-κB signaling in epithelial cells contributes to tumorigenesis by regulating expression of tumor-associated cytokines and anti-apoptotic genes. In models of colitis-associated cancer (78), gastric cancer (79), hepatocellular carcinoma (80), and melanoma (81), inhibition of NF-κB signaling in epithelial cells reduced tumor number/incidence and resulted in increased apoptosis of transformed epithelial cells. Our group has shown that long-term conditional activation of NF-κB signaling via IKKβ expression in airway epithelial cells results in increased lung inflammation, leading to an immunosuppressive lung microenvironment and formation of lung tumors, even in the absence of an additional oncogenic stimulus (82). In agreement, studies using

carcinogen, mutant-Kras, and mutant-EGFR lung tumor models have demonstrated that

NF-κB signaling in airway epithelial cells is crucial for tumorigenesis. Conditional

activation of NF-κB signaling in airway epithelial cells resulted in increased lung

inflammation and numbers of lung tumors induced by the complete lung carcinogen

urethane. Activation of NF-κB signaling was also associated with increased proliferation

and decreased apoptosis of epithelial cells (83). Conversely, expression of a dominant

inhibitor of NF-κB in lung epithelial cells of both mice treated with urethane and mice with

conditional expression of mutant EGFR in lung epithelial cells decreased lung

inflammation and tumor formation (84, 85). In urethane-treated mice with NF-κB

inhibition, decreased lung inflammation and tumor formation was associated with

increased epithelial cell apoptosis (84). In mice with oncogenic EGFR expression, NF-κB

inhibition reduced recruitment of pro-tumorigenic macrophages to the lung (85). A variety

of methods (blocking IκB degradation, knockdown of IKKβ, or p65/RelA deletion) have

been used to knock down epithelial NF-κB signaling in mutant-Kras lung cancer models.

Each of them found reduced lung tumors as well as increased apoptosis or decreased

proliferation of epithelial cells (86–88). Collectively, these studies strongly support

targeting the NF-κB signaling pathway for lung cancer treatment.

Targeting the NF-κB pathway in lung cancer

Over 780 agents have been identified that inhibit NF-κB signaling directly or

indirectly (89). These include antioxidants as well as inhibitors of upstream targets of

NF-κB, IKK and IκB phosphorylation, IκB degradation, proteasomes and proteases, NF-

κB nuclear translocation, NF-κB expression, NF-κB DNA binding, and NF-κB

transactivation (89). The proteasome inhibitor bortezomib is the most well-studied

inhibitor of NF-κB signaling. Bortezomib blocks signaling through the NF-κB pathway by

preventing proteosomal degradation of IκB. It received FDA approval in 2003 for the treatment of multiple myeloma (90) and has been involved in over 750 clinical trials as a therapeutic for numerous cancer types (ClinicalTrials.gov). While bortezomib increased sensitivity of human lung cancer cell lines to chemotherapy-induced apoptosis (91–93), bortezomib has not shown efficacy in NSCLC treatment. Bortezomib monotherapy in advanced NSCLC patients had limited activity in randomized phase I and II trials (94). When combined with chemotherapy or targeted therapy, bortezomib was well-tolerated but did not significantly affect tumor responses (95–102). Thus, a future role for bortezomib in lung cancer treatment is uncertain.

Several methods have been employed to investigate the effects of NF-κB inhibitor therapy in cell and animal models of lung cancer, showing variable results. Directly blocking NF-κB using siRNA, IKK inhibitors, and IκB super suppressors reduced cell survival and inhibited proliferation in lung cancer cell lines treated with chemotherapy or activators of TNF/TRAIL death receptor pathways (103–105). Similarly, indirect NF-κB inhibition using the flavonoids genistein and luteolin sensitized lung cancer cell lines to apoptosis induced by chemotherapy and gamma radiation, respectively (106, 107). In Kras-mutant mouse studies, Basseres et al. and Xue et al. showed short-term lung tumor responses to different NF-κB inhibitor therapies, including a specific IKKβ inhibitor (Cmpd A), bortezomib, and BAY 11-7082, an inhibitor of IκBα phosphorylation (108, 109). However, long-term responses with these agents were not observed. The IKKβ inhibitor was administered for only 4 weeks, and tumors developed resistance to bortezomib and BAY 11-7082 within 13 and 8 weeks of treatment, respectively (108, 109). Even more, our group has shown that lung tumor formation was enhanced, not hindered, in urethane-treated mice administered prolonged treatment with bortezomib (110). The mechanism of resistance to bortezomib and other NF-κB inhibitor therapies is not known. Though tumor cells could develop intrinsic resistance to NF-κB

inhibitors via the acquisition of additional mutations (109), this would likely translate into sporadic appearance of secondary resistance, as opposed to the uniform primary resistance to bortezomib observed in various solid tumors (101, 102). Alternatively, it is possible that separate cell types respond differently to NF-κB inhibition during tumorigenesis.

Myeloid Cells

Roles in innate immunity

The lungs are highly populated with innate immune cells known as myeloid cells that respond quickly to inhaled particulates and airborne pathogens (111). Myeloid cells are bone-marrow derived leukocytes, including neutrophils, macrophages, and dendritic cells, and employ a variety of mechanisms to maintain homeostasis in the lungs (**Figure 6**). Neutrophils are granulocytic cells that eliminate pathogens primarily by phagocytosis. Additionally, they may undergo respiratory burst, releasing granzymes and toxic reactive oxygen/nitrogen species. Macrophages and dendritic cells are phagocytic antigen-presenting cells, which activate T and B cells to initiate adaptive immune responses against specific antigens. Both macrophages and dendritic cells release inflammatory mediators and cytokines to regulate inflammation and immune responses. Like neutrophils, they are also capable of releasing toxic reactive oxygen species to defend against pathogens (112).
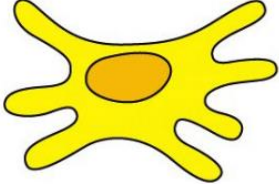
Cell type	Neutrophils	Macrophages	Dendritic cells
Function	Phagocytosis Reactive oxygen and nitrogen species Antimicrobial peptides	Phagocytosis Inflammatory mediators Antigen presentation Reactive oxygen and nitrogen species Cytokines Complement proteins	Antigen presentation Costimulatory signals Reactive oxygen species Interferon Cytokines

Figure 6: Functions of myeloid cells during innate immune responses.
Neutrophils, macrophages, and dendritic cells are innate myeloid cells that are first-responders to pathogens and other non-host antigens. Each cell type uses a variety of functions to eliminate foreign substances and recruit other innate and adaptive immune cells to mount a robust immune response. Figure modified and used with permission from Kuby Immunology (112). Table 3-12 in Kuby, IMMUNOLOGY, Sixth Edition © 2007 W.H. Freeman and Company.

Myeloid cells in cancer

Myeloid cells are characterized by remarkable plasticity, altering their phenotypes based upon signals received from the surrounding microenvironment. In the context of a tumor, myeloid cells have the ability to directly eliminate cancer cells and initiate anti-tumorigenic immune responses. However, these anti-tumorigenic responses are often thwarted by tumor cells themselves, which produce factors that polarize myeloid cells or prevent their differentiation so that myeloid cells support tumor growth and progression (113). Macrophages, neutrophils, dendritic cells, and myeloid-derived suppressor cells (MDSC) are all commonly found in the tumor microenvironment, polarized toward a tumor-favoring phenotype (114). Recently, macrophages and neutrophils have been heavily studied for their roles during tumorigenesis.

16

In 2002, Mantovani et al. introduced a simplistic paradigm for classically-activated M1 and alternatively-activated M2 macrophage polarization states based on expression of cell surface markers and cytokines (115) (**Figure 7)**. Th1 cytokines and/or microbial components (LPS) induce macrophage polarization towards the M1 phenotype. M1 macrophages mount classic Th1 immune responses, supporting resistance to microbes and tumor cells. They produce high levels of IL-12, IL-23, ROS, RNS, and inflammatory cytokines (e.g. IL-1β, TNF, and IL-6) (113). In contrast, Th2 cytokines, such as IL-4 and IL-13, inhibit classical macrophage activation and instead induce alternative activation of macrophages. Alternatively-activated M2 macrophages highly express the immunosuppressive cytokine IL-10, tumor growth factors (e.g. EGF, FGF1, TGFβ1), pro-angiogenic factors (VEGF), matrix remodeling factors (e.g. fibrin and MMPs), and chemokines involved in recruitment of Th2 cells and immunosuppressive regulatory T cells (Tregs) (CCL17, CCL22, CCL24) (113). They play roles in resolution of inflammation, wound healing, angiogenesis, and tissue remodeling (113). Macrophages present in or surrounding a tumor are called tumor-associated macrophages (TAM). Several experimental studies indicate that TAM have an M2-like phenotype and promote tumor formation and progression through angiogenesis, immunosuppression, and perpetuation of cancer-associated inflammation (115–118).
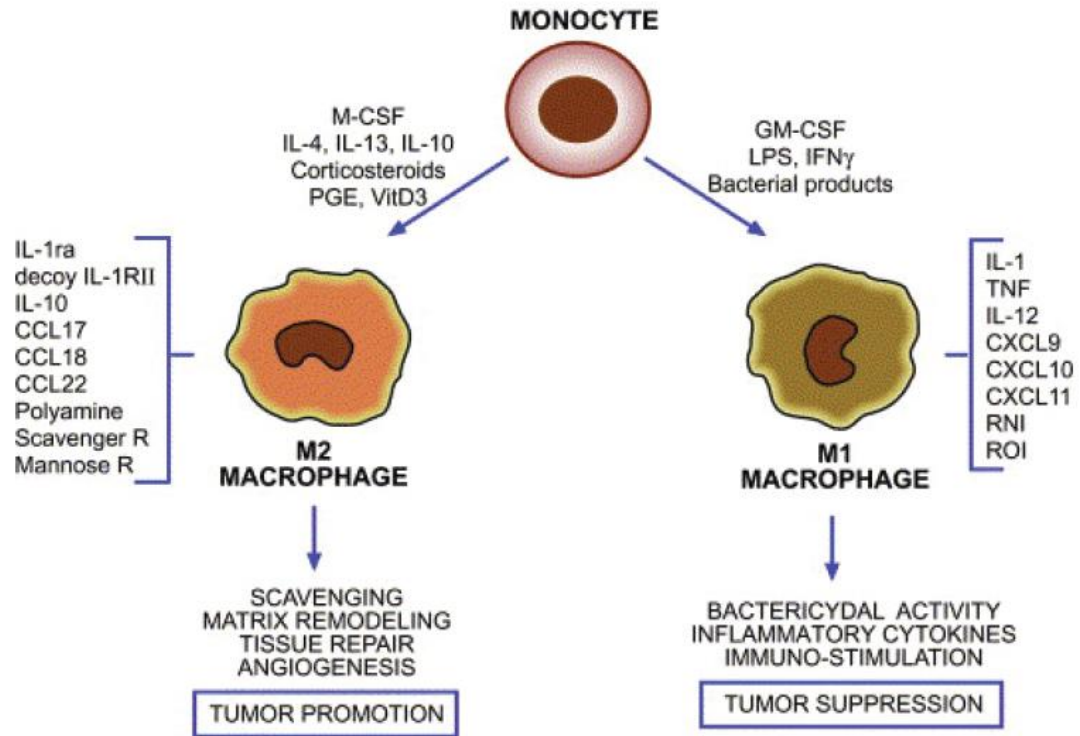
Figure 7: Polarization of macrophages to anti-tumorigenic M1 or pro-tumorigenic M2 phenotypes.

Monocytes are differentiated into two broad phenotypes based on signals they receive from the microenvironment. Left: Stimuli that induce the tumor-promoting M2 phenotype include M-CSF, IL-4, IL-13, IL-10, corticosteroids, PGE, and vitamin D3. M2 macrophages highly express immunosuppressive cytokines, Th2 chemokines, and matrix remodeling factors that promote tumors through scavenging, matrix remodeling, tissue repair, and angiogenesis. Right: The M1 phenotype is induced by GM-CSF, LPS, IFNγ, and bacterial products. Anti-tumorigenic M1 macrophages secrete Th1 pro-inflammatory cytokines and chemokines as well as reactive oxygen and nitrogen intermediates (ROI and RNI, respectively) to elicit bactericidal activity, heightened immune responses, and tumor suppression. Reprinted from European Journal of Cancer, Volume 42, Issue 6, Sica A, Schioppa T, Mantovani A, Allavena P. Tumour-associated macrophages are a distinct M2 polarised population promoting tumour progression: potential targets of anti-cancer therapy. 717-727, Copyright(2016), with permission from Elsevier(119).

The role of TAMs during lung tumorigenesis in NSCLC patients is controversial but seems to be dependent on both localization and phenotype. Several studies have observed a survival benefit in NSCLC patients whose tumors had a high density of macrophages (120–122). Further investigation discovered that 70% of macrophages

present in lung tumors were of the M1 phenotype, and M1 macrophage density in tumors independently predicted increased survival in NSCLC patients (123, 124). In contrast, increased macrophage density in the tumor stroma was associated with reduced survival (122). One study found that in advanced NSCLC, more than 95% of TAMs were located in the tumor stroma and identified as M2-like macrophages. M2 macrophages were higher in patients with progressive disease (125). This finding was confirmed in other studies showing that increasing M2 macrophage density correlated with poor prognosis in NSCLC patients (126, 127).

In addition to macrophages, an N1/N2 paradigm has been proposed by Fridlender et al. for neutrophils, with N1 and N2 neutrophils having anti- and pro-tumorigenic properties, respectively (**Figure 8**). The N1 phenotype is induced by IFNβ (128, 129). N1 neutrophils have hypersegmented nuclei and express high levels of immune-activating cytokines and chemokines, adhesion molecule ICAM1, and death receptor Fas (130). N1 neutrophils directly kill tumor cells using ROS-mediated tumor cell lysis (130–132) or by inducing Fas ligand-associated apoptosis (133). Through chemokine and cytokine secretion, N1 neutrophils also recruit and activate CD8^{+} and CD4^{+} T cells to kill tumor cells and mediate anti-tumoral memory, respectively (130, 134–137). Expression of TGFβ by tumors induces recruitment of neutrophils to the tumor via expression of neutrophil chemoattractant chemokines (CXCL2, CXCL5, and CCL3) and polarizes tumor-associated neutrophils (TAN) towards the N2 phenotype (130). N2 TANs have circular nuclei, expressing high levels of arginase, CCL2, and CCL5 (130) and generating low amounts of neutrophil granules and ROS (138). Arginase produced by N2 neutrophils inactivates T cells and facilitates pro-tumorigenic immunosuppression (139, 140). The chemokines CCL2 and CCL5 produced by N2 TANs also promote tumorigenesis by supporting cancer cell proliferation, angiogenesis, and immunosuppression (141–143).
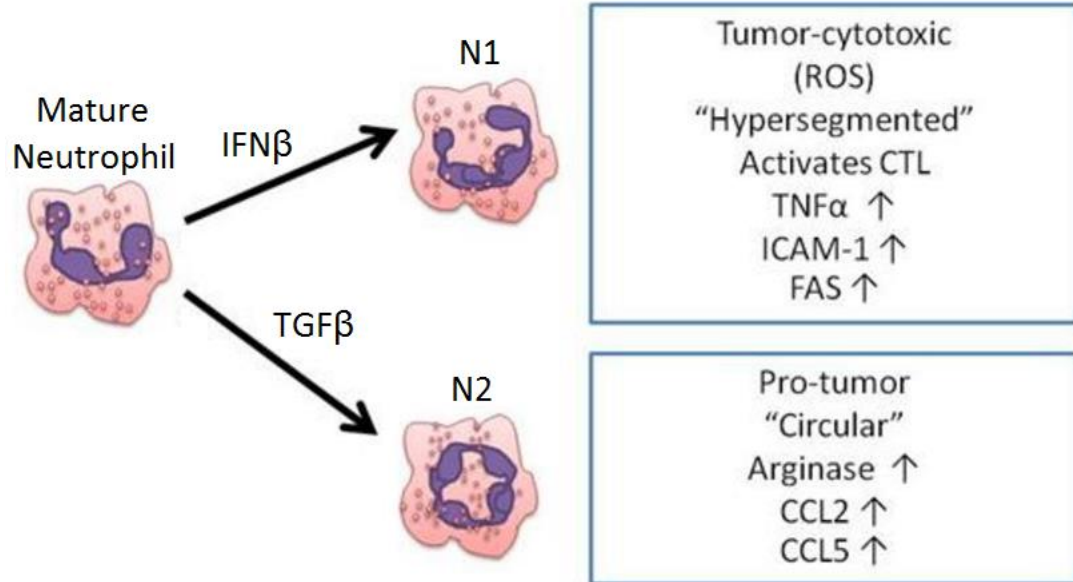
Figure 8: Polarization of neutrophils to anti-tumorigenic N1 or pro-tumorigenic N2 phenotypes.
Neutrophils are polarized toward anti-tumorigenic N1 neutrophils by IFNβ and toward pro-tumorigenic N2 neutrophils by TGFβ. N1 neutrophils are cytotoxic to tumors and express high levels of TNFα, ICAM1, and FAS. They also activate T cells to stimulate a robust anti-tumor immune response. N2 neutrophils express high levels of arginase, CCL2, and CCL5, which promote tumor growth, support angiogenesis, and/or mediate immunosuppression.
Figure modified from Thanee et al. (144), which modified from Fridlender et al. (138). Fridlender ZG, Albelda SM. Tumor-associated neutrophils: friend or foe?. *Carcinogenesis.* 2012;33(5):949–955 by permission of Oxford University Press.

The role of TANs during lung tumorigenesis is complex and, like TAMs, appears to depend on localization and phenotype. Elevated circulating neutrophil counts have been associated with a worse prognosis in advanced NSCLC patients (145–148). Neutrophils at the tumor site tend to have an N2 phenotype as a result of TGFβ expression by the tumor (149). CD66b⁺ N2-like TANs are elevated in 50% of resectable NSCLC tumors and have been associated with high incidence of relapse and worse overall survival (150). On the other hand, another group described an immunostimulating N1-like role for TANs in early-stage lung cancer rather than an immunosuppressive role (151). Thus, much remains to be elucidated concerning the roles of TANs in NSCLC patients.

Myeloid-derived suppressor cells (MDSCs) are a heterogeneous mixture of immature monocytic and granulocytic myeloid cells that are increased in NSCLC and are associated with angiogenesis (152, 153), tumor progression (154), metastatic spread (155), and poorer outcomes (156). In mice, MDSCs are identified by positive expression of the cell surface markers CD11b and Gr1; in humans, MDSCs are identified using positive expression of CD11b and CD33 along with low or absent expression of HLA DR (157–160). MDSCs exert their pro-tumorigenic effects by inhibiting the function of effector and antigen presenting cells in the tumor microenvironment (160–162). MDSCs express PD-L1, which binds to PD-1 on the surface of T effector cells and inactivates them (163). Arginase-1 produced by MDSCs induces cell cycle arrest of T effector cells (164–166) and inhibits proliferation and secretion of IFNγ by natural killer cells (167). Expression of iNOS and ROS by MDSCs results in the generation of reactive nitrogen species, such as NO (164, 165). NO has been shown to suppress T cell function via the JAK/STAT signaling pathway (168), reducing MHC expression (169), disrupting the TCR (170, 171), and inducing T cell apoptosis (172). Finally, expression of IL-10 by MDSCs induces polarization of T cells to the immunosuppressive Treg phenotype (173, 174) and macrophages to the immunosuppressive M2 phenotype (175).

Inhibition of NF-κB in myeloid cells during tumorigenesis

Several studies have investigated the impact of NF-κB inhibition in myeloid cells on tumorigenesis, yielding controversial findings. Blocking myeloid cell-specific NF-κB signaling reduced colon tumors and tumor-promoting cytokines in the azoxymethane dextran sulfate sodium salt model of colitis-associated carcinoma (78). Similarly, Takahashi et al. showed that inhibition of myeloid NF-κB signaling reduced lung tumors in Kras-mutant mice in response to tobacco smoke exposure. In this model, myeloid NF-

κB inhibition also reduced lung inflammation, cytokine expression, and proliferation (176). The mechanism responsible for these anti-tumorigenic responses may be through induction of classic innate immune responses in TAMs. Blocking NF-κB signaling in TAMs has been shown to induce an anti-tumorigenic M1 phenotype that is able to promote tumor regression through induction of tumoricidal activity and recruitment of natural killer cells (177, 178). In contrast to these beneficial responses to myeloid-specific NF-κB inhibition, blocking the signaling in cutaneous and lung melanoma models rapidly induced tumor growth. Myeloid cells with inhibited NF-κB signaling had reduced phagocytic ability and thus could not effectively eliminate tumor cells (179). Additionally, myeloid cell-specific NF-κB inhibition in a melanoma chemotherapy model resulted in increased tumor necrosis and mortality instead of tumor regression in response to doxorubicin. Tumors in mice with inhibited NF-κB signaling were rapidly populated by IL-1β-producing neutrophils, which sustained inflammation and facilitated necrosis (180). Thus, the effect of NF-κB inhibition in myeloid cells on carcinogenesis seems to be organ and/or context-dependent. Further study is necessary to understand differential responses to myeloid cell-specific NF-κB inhibition in different cancer models.

Summary and dissertation goals

The American Cancer Society estimated that over 220,000 Americans would be diagnosed with lung cancer in 2015, and another 158,000 would die from this disease (3). Despite significant advances in personalized therapy for lung cancer patients with targetable driver mutations in their tumor cells, benefits from each targeted therapy administered last at most a few months, and patients will eventually succumb to their disease as a result of tumor resistance to therapy (41, 53). In recent years, targeting cancer-related inflammation and modulating the immune system has received attention

as a potential alternative approach to treating lung and other cancers (54). The NF-κB pathway is a master regulator of inflammation and is activated in most cancers, including lung cancer. While it is known to play critical roles in promoting proliferation and survival of mutated lung epithelial cells, treatment of NSCLC patients with NF-κB inhibitors has not been effective. Myeloid cells are highly plastic cells that can be polarized toward anti- or pro-tumorigenic phenotypes in response to different signals from the microenvironment. The role of NF-κB signaling in myeloid cells during carcinogenesis is not fully understood, and it appears to be organ- and/or context-dependent.

The goals of this dissertation were to determine the role of NF-κB signaling in myeloid cells during lung tumorigenesis and to identify novel therapeutic targets for the treatment of NSCLC. Our studies demonstrate that inhibition of NF-κB specifically in myeloid cells results in enhanced lung inflammation and tumorigenesis, providing a rationale for why NF-κB-targeted therapies are ineffective for lung cancer treatment. We determined that pro-IL-1β processing by neutrophils is a critical pathway of immune-mediated chemoresistance to NF-κB inhibitors, which can be overcome using combination therapy with inhibitors of NF-κB and IL-1 signaling. Collectively, our findings show that NF-κB inhibitors are ineffective for lung cancer therapy due to the pro-tumorigenic effects of NF-κB inhibition in myeloid cells. Our studies suggest that combined biological interventions targeting the NF-κB pathway and myeloid cell-derived pro-tumorigenic mediators could be beneficial in lung cancer patients.

CHAPTER II: MATERIALS AND METHODS

Ethics statement

All animal care and experimental procedures were approved and conducted according to guidelines issued by the Vanderbilt University Institutional Animal Care and Use Committee. Human de-identified plasma samples from a phase II clinical trial of advanced NSCLC patients were a kind gift from Dr. Vassilis Georgoulias at the University General Hospital of Heraklion in Crete, Greece.

Patient samples

Twenty-eight chemotherapy-naïve patients with inoperable, locally-advanced (Stage IIIB) or metastatic (Stage IV) NSCLC were treated with bortezomib (1 mg/m^2) as part of a phase II clinical trial performed at the University Hospital of Crete (Protocol NCT01633645). Bortezomib was administered alone for the first cycle of treatment. All subsequent treatment cycles contained bortezomib plus gemcitabine and cisplatin. Plasma samples were collected before, 1 hour, and 24 hours after the first dose of bortezomib (Day 0) as well as before and 24 hours after the second dose of bortezomib (Day 8).

Mice

Mice used for studies were 8 to 10 weeks old and both age- and sex-matched.

IKKβ^{Δmye} mice (IKKβ$^{fl/fl}$; LysM-Cre) on the C57BL6/J background (181) were backcrossed to the FVB genetic background for 10 generations. Lung tumors in these mice were

induced by a single intraperitoneal (IP) injection of urethane (ethyl carbamate, 1 g/kg; Sigma-Aldrich, St. Louis, MO). Littermate IKKβ$^{fl/fl}$ mice with wild-type (WT) NF-κB signaling (called WT in our studies) were used as controls. BAY 11-7082 (Cayman Chemical, Ann Arbor, MI) was delivered by IP injection at 10 mg/kg body weight as described (109), and bortezomib (Millenium, Cambridge, MA) was delivered by IP injection at 1 mg/kg as previously described (110). Mice were sacrificed at 1, 6, and 16 weeks after urethane injection.

LSL-Kras^{G12D} mice on the C57BL6/J background (182) were backcrossed to the FVB genetic background for 10 generations. Lung tumors in these mice were induced using intratracheal (IT) injection of adeno-Cre (1.5 x 10^7 PFU, University of Iowa Carver College of Medicine). Mice were harvested at 8 weeks after adeno-Cre.

Doxycycline (Dox)-inducible Kras^{G12D} mice that express mutant Kras^{G12D} in Clara cell secretory protein (CCSP)-positive airway epithelial cells [CCSP-rtTA (tet-O)- Kras^{G12D}] were used for treatment studies (183). Lung tumors were established in these mice via consumption of dox (0.5 g/L) in drinking water for 4 weeks. Subsequently, mice were treated with dox plus bortezomib, IL-1 receptor antagonist (IL-1ra, also known as anakinra/Kineret®, 60 mg/kg/d; Amgen, Thousand Oaks, CA), bortezomib plus IL-1ra, or vehicle control for 4 weeks.

Caspase-1 knockout (Casp1 KO) mice on the C57BL/6 background (B6N.129S2-Casp1^{tm1Flv}/J) were obtained from The Jackson Laboratory (Bar Harbor, ME). Lung tumors in Casp1 KO mice and WT C57BL/6 controls were induced by 4 weekly IP injections of urethane (1 g/kg) as previously described (84). Mice were euthanized at 4 months after the first injection of carcinogen.

NF-κB reporter mice on the FVB genetic background were generated in our laboratory and express a green fluorescent protein (GFP)-luciferase fusion protein upon expression of an NF-κB-dependent promoter (184). When injected retro-orbitally with luciferin, NF-κB activation can be detected using bioluminescent imaging.

Bioluminescent imaging

NF-κB reporter mice (184) were anesthetized and shaved over the chest prior to imaging. Luciferin (1 mg/mouse in 100 μL isotonic saline) was injected retro-orbitally, and mice were placed inside of a light-tight box housing an intensified charge-coupled device (ICCD) camera (IVIS 200; Xenogen, Alameda, CA) for imaging. Light emission from the mouse was detected as photon counts by the ICCD camera and customized with image processing hardware and software (Living Image software; Xenogen). The imaging duration selected was 30 s to prevent saturation of the camera during image acquisition. To perform quantitative analysis, a standard area over the mid-lung zone was defined, and the total integrated photon intensity over the area of interest was measured.

Cell lines

The murine Lewis lung carcinoma (LLC) cell line was purchased from American Tissue Culture Collection (ATCC, Rockville, MD). Cells were cultured in Dulbecco's Modified Eagle Medium (DMEM; Gibco, BRL, Carlsbad, CA) supplemented with 10% fetal bovine serum (FBS; Sigma-Aldrich) and 1% penicillin-streptomycin (Pen Strep; Mediatech, Inc., Manassas, VA) at 37°C and 5% CO_2.

Subcutaneous tumor formation and monitoring

To establish subcutaneous tumors, 250,000 murine LLC cells were injected subcutaneously into the flanks of syngeneic C57BL/6 mice. Tumors were allowed to grow to a volume of 10 mm^2, upon which treatment with bortezomib, IL-1ra, bortezomib plus IL-1ra, or vehicle control was initiated. Tumor volume was monitored every two days. For tumor volume, length and width measurements were obtained using Traceable digital calipers (Fisher Scientific), and volume was calculated using the formula $V = \frac{\pi}{6} f(length \cdot width)^{\frac{3}{2}}$ as previously described (185).

Bronchoalveolar lavage (BAL)

BAL was performed by flushing the lungs 3 times with 800 μL phosphate buffered saline (PBS). Total cell count was determined using a grid hemocytometer. Cell differentials were determined by counting 300 cells per Wright-Giemsa-stained cytocentrifuged slide.

Histology

At the time of sacrifice, lungs were perfused with PBS and fixed in 10% formalin (Thermo Fisher Scientific, Waltham, MA) or Bouin's fixative solution (Sigma-Aldrich). After 24 hours of fixation, lungs were used for surface tumor counting and diameter measurements under a dissecting microscope by at least two experienced readers blinded to sample identifiers. Tumor diameters were measured using Fisherbrand Traceable digital calipers (Fisher Scientific). Lungs were then embedded in paraffin,

27

sectioned (5 µm), stained with hematoxylin and eosin (H&E), and analyzed by a pathologist blinded to the experimental groups for evaluation of tumor and atypical adenomatous hyperplasia (AAH) lesions in 3 separate sections cut at predetermined depths.

Immunohistochemistry

For proliferation and apoptosis analyses, lung sections were immunostained with antibodies against proliferating cell nuclear antigen (PCNA; Life Technologies, Carlsbad, CA) or cleaved caspase-3 (Cell Signaling, Beverly, MA). Proliferation and apoptosis indices were calculated by counting the number of positive cells per 40x field and averaged from 25 randomly chosen fields. For analysis of tumor-infiltrating blood vessels, lung sections were immunostained with anti-CD34 antibodies (clone MEC14.7; BioLegend, San Diego, CA). Blood vessel density in tumors was calculated as the number of CD34$^+$ endothelial cells per square millimeter of tumor area.

Lung single cell suspensions

Lungs were perfused with PBS and digested in Roswell Park Memorial Institute (RPMI) medium (Gibco) supplemented with collagenase XI (0.7 mg/mL; Sigma-Aldrich) and type IV bovine pancreatic DNase (30 µg/mL; Sigma-Aldrich) for 40 minutes at 37°C. Digested lungs were homogenized through a 70 µm cell strainer to obtain single-cell suspensions. Treatment with RBC Lysis Buffer (BioLegend) was used to remove red blood cells.

Flow cytometry/Fluorescence-activated cell sorting (FACS)

Single-cell suspensions were incubated with Fc receptor block (1 µg/1 x 10^6 cells; BD Biosciences, Franklin Lakes, NJ) to reduce nonspecific antibody binding. The panel of antibodies used in these experiments included: CD45 - APC-Cy7, CD11b - V450, Gr1 - PerCP-Cy5.5 (all from BioLegend); Ly6C - FITC and Ly6G - PerCP-Cy5.5 (BD Biosciences); CD4 - FITC and CD25 - APC (e-Bioscience, San Diego, CA); MPO - FITC (Abcam, Cambridge, MA). Cells were stained with 4′,6-diamidino-2-phenylindole (DAPI; Life Technologies) to exclude dead cells from analysis. Flow cytometry was performed using the BD LSR II flow cytometer (BD Biosciences), and data were analyzed with FlowJo software (TreeStar, Ashland, OR). For *in vitro* studies, CD11b$^+$ cells were purified by magnetic separation using microbeads (Miltenyi Biotec, San Diego, CA) followed by FACS based on expression of Ly6G and Ly6C.

Allogenic Mixed Leukocyte reaction (MLR) assay

CD4$^+$/CD25$^-$ effector T cells (Teff) were isolated from spleens of naïve FVB mice (1 x 10^5/well) and labeled with carboxyfluorescein succinimidyl ester (CFSE) fluorescent dye (5 µM; Life Technologies, Carlsbad, CA) to measure cell proliferation in response to allogeneic mature bone marrow-derived dendritic cells from C57BL/6 mice. Dendritic cells were generated by culturing bone marrow cells in DMEM (Gibco) supplemented with 10% FBS (Sigma-Aldrich), 1% Pen Strep (Mediatech), 2-ME (50 mM; Gibco), recombinant granulocyte macrophage colony-stimulating factor (GM-CSF) (20 ng/mL; Miltenyi Biotec), and interleukin 4 (20 ng/mL; Miltenyi Biotec) for 7 days. Dendritic cells were matured starting on day 7 by incubation for 24 hours with lipopolysaccharide (LPS) (1 µg/mL; Sigma-Aldrich). The ratio between the dendritic cells and CD4$^+$/CD25$^-$ Teff

cells was 1:10. The suppressive function of CD11b$^+$/Ly6G$^+$ lung neutrophils from IKKβ^{Δmye} mice was tested on the proliferation of CFSE-labeled Teff cells by flow cytometry. Dead cells were excluded from analysis based on staining with DAPI.

Real-time polymerase chain reaction (RT-PCR)

RNA from whole lung tissue or sorted myeloid cells was isolated using the RNeasy Mini kit (Qiagen, Valencia, CA). cDNA was generated using SuperScript III Reverse Transcriptase (Life Technologies) and then subjected to RT-PCR using SYBR Green PCR Master Mix (Life Technologies) and the StepOnePlus^{TM} RT-PCR System (Applied Biosystems, Grand Island, NY). Relative mRNA expression in each sample was normalized to GAPDH and presented using the comparative Ct method ($2^{ΔCt}$). Primer sequences utilized are listed in **Table 1**.

Gene	Forward Primer (5'→3')	Reverse Primer (5'→3')
G-CSF	TTGGTGAGTGGGGTTGCCATAGGT	TGCCCTCTTCTCATTTGTGCTCCT
GM-CSF	CGTTGGTGAGTGAGGGAGAGAGTT	TGAAAGGCAGGGCAAGACAAGG
IL-6	AAAGAGTTGTGCAATGGCAATTCT	AAGTGCATCATCGTTGTTCATACA
KC	CCGAAGTCATAGCCACACTCAA	GCAGTCTGTCTTCTTTCTCCGTTAC
IL-1β	GCAACTGTTCCTGAACTCAACT	ATCTTTTGGGGTCCGTCAACT
CatG	GCCAATCGCTTCCAGTTCTAC	GTGGGTGTTCACATTCTTACCC
TNFα	AAGCCTGTAGCCCACGTCGTA	GGCACCACTAGTTGGTTGTCTTTG
IL-12p35	TGGACCTGCCAGGTGTCTTAG	CAATGTGCTGGTTTGGTCCC
ICAM1	TGCCTCTGAAGCTCGGATATAC	TCTGTCGAACTCCTCAGTCAC
IFNγ	GCGTCATTGAATCACACCTGA	CTCGGATGAGCTCATTGAATGC
iNOS	CACCTTGGAGTTCACCCAGT	ACCACTCGTACTTGGGATGC
CCL2	TTAAAAACCTGGATCGGAACCAA	GCATTAGCTTCAGATTTACGGGT

CCL5	ACCATGAAGATCTCTGCAGC	TGAACCCACTTCTTCTCTGG
CCL17	TGCTTCTGGGGACTTTTCTG	CATCCCTGGAACACTCCACT
VEGF	TTACTGCTGTACCTCCACC	ACAGGACGGCTTGAAGATG
IL-10	ACCTGCTCCACTGCCTTGCT	GGTTGCCAAGCCTTATCGGA
Arg1	GATTGGCAAGGTGATGGAAG	TCAGTCCCTGGCTTATGGTT
GAPDH	TGAGGACCAGGTTGTCTCCT	CCCTGTTGCTGTAGCCGTAT

Table 1: Primer sequences for detection of cytokines and chemokines in mouse tissue using real-time PCR.

Cytokine protein expression

G-CSF, GM-CSF, IFNγ, IL-4, IL-6, IL-10, IL-12p40, KC, CCL2, and CCL3 protein concentrations were measured in whole lung homogenates by the MILLIPLEX MAP Mouse Cytokine/Chemokine Panel (Millipore, Billerica, MA) and analyzed with MILLIPLEX® Analyst software (Millipore). Murine IL-1β protein was measured in whole lung homogenates and conditioned media by ELISA (R&D Systems, Minneapolis, MN). Murine vascular endothelial growth factor (VEGF) was measured in BAL fluid by ELISA (R&D Systems). Human plasma IL-1β, IL-8, and TNF were measured using the BD™ Cytometric Bead Array Human Enhanced Sensitivity Flex Sets (limits of detection were 48.4 fg/mL, 69.9 fg/mL, and 67.3 fg/mL, respectively) (BD Biosciences), and IL-6 was measured using the BD™ Cytometric Bead Array Human Flex Set (limit of detection was 1.6 pg/mL) (BD Biosciences).

Bone marrow cell isolation

Femurs were removed from mice and washed in ice cold PBS. The tips of the femurs were cut off, and the marrow was flushed out of each bone using a 10mL syringe

of PBS and a 25-gauge needle. After centrifugation, red blood cells were lysed using RBC Lysis Buffer (BioLegend).

Western blot

Whole cell lysates were prepared using CelLytic™ MT Cell Lysis Reagent (C3228; Sigma), separated by SDS-PAGE gel, transferred to nitrocellulose membrane, and probed with anti-IKKβ (10AG2; Novus Biologicals) and anti-β-actin (A5316; Sigma). Immunodetection was performed using the corresponding AlexaFluor-conjugated antibodies and the Odyssey Infrared Imaging System (LI-COR Biosciences).

Bone marrow transplantation

For transplantation studies, lethally-irradiated (9.5 Gy) recipient mice were injected with bone marrow cells (2×10^6 bone marrow cells/mouse in PBS) from sex-matched, syngeneic donor mice. The recipient chimeric animals were then housed under specific pathogen-free (SPF) conditions with access to autoclaved food and pH2 water containing neomycin (100 mg/L; Sigma-Aldrich) and polymyxin B (10 mg/L; Sigma-Aldrich). To deplete resident lung macrophages, reconstituted chimeras were anesthetized, intubated using a 1 mL syringe with a 6 mm-long, 22-gauge, over-the-needle catheter (Abbocath-T, Venisystems, Mundelein, Illinois), and injected IT with 100 µl of liposomal clodronate (dichloromethylene diphosphonic acid, Sigma-Aldrich) at 4 weeks after transplantation. Chimeras were then housed under SPF conditions and used for lung tumor studies 3 weeks later.

Depletion or neutralization of neutrophils, macrophages, and IL-1ra

For neutrophil depletion, 100 µg of anti-Ly6G antibodies (Clone 1A8, BioLegend) or IgG2a isotype control antibodies (BioLegend) were delivered by IP injection twice a week for the first six weeks after urethane injection. For macrophage depletion, liposomal clodronate (dichloromethylene diphosphonic acid, Sigma-Aldrich) or liposomal phosphate buffered saline (PBS) was delivered by IT injection as previously described (186). To block IL-1β signaling, mice were treated with IL-1ra or PBS (vehicle control) delivered by subcutaneously implanted Alzet osmotic pumps (DURECT Corp., Cupertino, CA) with an infusion rate of 0.5 µL/h for 2 weeks. After 2 weeks, osmotic pumps were replaced to complete a 4-week course of treatment. Pumps were loaded such that each mouse received 60 mg/kg/day of IL-1ra.

In vitro inhibitor studies

Equal numbers of neutrophils were seeded into 96-well plates. Cells were cultured for 1 hour in the presence of caspase-1 inhibitor Ac-YVAD-CMK (100 µM; N-1330.0005; Bachem), neutrophil elastase and proteinase 3 inhibitor MeOSuc-APPV-CMK (100 µM; CAS 65144-34-5; Santa Cruz Biotechnology), or cathepsin G inhibitor Z-GLP-CMK (100 µM; 03CK00805; MP Biomedicals).

Statistical analysis

Data from mouse models were analyzed using the GraphPad Prism 5.0 software (GraphPad Software Inc., La Jolla, DA), and values are presented as mean ± SEM. Pair-wise comparisons were made using Student's t-tests. For experiments conducted over

several time points or with multiple comparisons, a two-way ANOVA with a Bonferroni post-test was used to determine differences among groups. $p < 0.05$ was considered statistically significant.

Data from the 28 chemotherapy-naïve NSCLC subjects were analyzed using R software version 3.1.2 (www.r-project.org) and are expressed as median (interquartile range) for continuous variables and frequencies (proportions) for categorical variables. IL-1β, IL-8, TNF, and IL-6 before and 24 hours after initial treatment were compared using Student's t-test. Spearman correlation between baseline IL-1β and progression-free survival time in months was analyzed. We further applied a multivariable linear regression model to adjust for both subjects' age at baseline and performance status. Normality of residuals of the linear model was diagnosed, and log transformation on progression-free survival time was performed to correct non-normal residuals if needed. $p < 0.05$ was considered statistically significant.

CHAPTER III: INHIBITION OF NF-KB SIGNALING IN MYELOID CELLS ENHANCES

LUNG TUMORIGENESIS VIA IL-1β SIGNALING.

The contents of this chapter have been published and are shared with permission under
the CC BY-ND license (http://creativecommons.org/licenses/by-nc-nd/4.0/)

Rationale

The NF-κB pathway has become increasingly appreciated for its involvement in
carcinogenesis as studies continue to uncover its roles in primary tumor growth,
angiogenesis, and metastasis (187). In the lungs, NF-κB is activated in pre-malignant
airway epithelial lesions, atypical adenomatous hyperplasia (AAH) lesions in the distal
lungs, and invasive non-small cell lung cancer (NSCLC) (67). Based on this information,
inhibition of the NF-κB pathway has been tested as a therapy for lung cancer (188). The
proteasome inhibitor bortezomib, which blocks degradation of the inhibitor of NF-κB (IκB)
as well as other proteins that are regulated by the proteasome, is the best-studied agent
for inhibiting NF-κB in humans; however, bortezomib has not been efficacious for NSCLC
treatment (101, 102). The mechanism of resistance to bortezomib and other NF-κB
inhibitor therapies is not known. Despite the disappointing results to date, numerous
clinical trials have been attempted or are currently under way to test various combinations
of bortezomib and other agents for cancer treatment. Our goals for these studies were to
determine why NF-κB inhibitors are ineffective for NSCLC and to identify new approaches
to overcome resistance to NF-κB inhibitors.

Our group and others have shown that NF-κB signaling in lung epithelial cells is
crucial for lung tumor formation. In mice, expression of a constitutively active form of IKKβ
(which activates canonical NF-κB) in airway epithelium results in a >3-fold increase in lung
tumor formation after treatment with chemical carcinogens (83). In addition, a variety of
methods (blocking IκB degradation, knockdown of IKKβ, or p65/RelA deletion) have been

35

used to inhibit NF-κB signaling in lung epithelium and have revealed a requirement for NF-κB signaling in genetic and carcinogen-induced models of lung adenocarcinoma resulting from oncogenic *Kras* expression (84, 86–88). While some studies have shown short-term lung tumor responses to NF-κB inhibition (108, 109), pharmacologic NF-κB inhibition has not shown definitive long-term benefit in lung cancer models. Highlighting the challenges of NF-κB inhibition, Xue et al. showed that murine lung tumors developed resistance to therapy within a few weeks after treatment with bortezomib or an inhibitor of IκBα phosphorylation (BAY 11-7082) (109). Additionally, we showed that prolonged treatment with bortezomib enhanced, not hindered, lung tumor formation in urethane-treated mice (110). While it is possible that tumor cells could develop intrinsic resistance to NF-κB inhibitors via the acquisition of additional mutations (109), this would likely translate into sporadic appearance of secondary resistance, as opposed to the uniform primary resistance to bortezomib observed in various solid tumors (101, 102). Based on these observations, we postulated that systemic NF-κB inhibition evokes a pro-tumorigenic response from a non-epithelial cell population that overrides the anti-tumor effects resulting from NF-κB inhibition in epithelial cells.

Myeloid cells play important roles in both innate immunity and tumorigenesis (186, 189, 190). It is now well-accepted that macrophages and neutrophils can act as pro- or anti-tumorigenic cells during tumorigenesis depending on signals that they receive from the tumor and the tumor stroma (113, 138). The role of NF-κB signaling in these cells during tumorigenesis is controversial and seems to be organ- and/or context-dependent. Some cancer models show that blocking NF-κB signaling in myeloid cells elicits a protective, anti-tumorigenic response (78, 176). Others show that myeloid-specific NF-κB inhibition is detrimental and pro-tumorigenic (179, 180). In tumor-associated macrophages, blocking NF-κB can result in an anti-tumorigenic phenotype (177, 178). On

36

the other hand, a recent study showed that blocking NF-κB signaling in macrophages impedes their ability to mount anti-tumorigenic responses against melanoma cells (179).

For these studies, we postulated that inhibition of NF-κB signaling in myeloid cells could elicit pro-tumorigenic responses that limit the effectiveness of global (systemic) NF-κB inhibition. To test this hypothesis, we utilized a mouse model characterized by myeloid cell-specific deletion of IKKβ (IKKβ$^{\Delta mye}$ mice; LysM-Cre/IKKβ$^{flox/flox}$) (181). Although these mice lack canonical NF-κB signaling in myeloid cells, including macrophages and neutrophils, in some settings they have enhanced inflammatory responses (191). In carcinogen-induced and genetic lung cancer models, we found that blocking NF-κB signaling in myeloid cells enhances lung tumorigenesis through neutrophil-dependent production of IL-1β and that combined NF-κB and IL-1β targeted treatments reduces tumor formation and growth.

<center>Results</center>

Neutrophils enhance lung tumorigenesis when NF-κB is inhibited in myeloid cells

To determine the role of NF-κB signaling in myeloid cells during lung tumorigenesis, IKKβ$^{\Delta mye}$ mice were fully back-crossed (>9 generations) to the tumor-susceptible FVB background. Deletion of IKKβ in myeloid cells in the bone marrow compartment was confirmed by western blot (**Figure 9**).
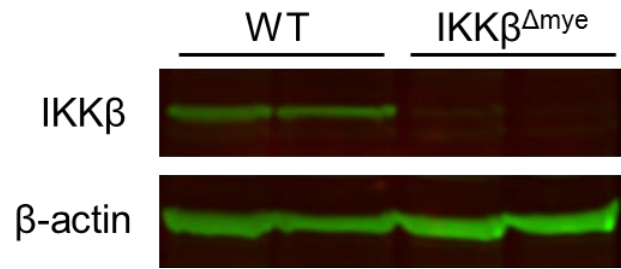
Figure 9: IKKβ is deleted in bone marrow cells of IKKβ^{Δmye} mice. Expression of IKKβ protein by western blot in bone marrow cells from WT and IKKβΔmye mice showing deletion of IKKβ in IKKβΔmye mice.

Subsequently, IKKβ^{Δmye} mice and WT littermate controls were given a single IP injection of the carcinogen urethane (1 g/kg). Urethane causes lung tumors primarily through induction of *Kras* mutations (192), but it can also induce a number of other driver mutations found in human cancers (193). At week 16 after injection of urethane, we found that IKKβ^{Δmye} mice developed approximately twice as many lung tumors as WT mice (**Figure 10A-B**), indicating that inhibiting NF-κB signaling in myeloid cells promotes lung tumorigenesis. To determine if differences were detectable at an earlier stage of carcinogenesis, we harvested lungs at 6 weeks after urethane injection and identified a greater number of AAH lesions in lungs of IKKβ^{Δmye} mice compared to WT mice (**Figure 10D**). Unexpectedly, at 6 weeks post-urethane, we observed some fully formed tumors in the lungs of IKKβ^{Δmye} mice (**Figure 10C**). On lung sections, 58% (7/12) of IKKβ^{Δmye} lungs contained adenomas at 6 weeks post-urethane compared with 7.1% (1/14) of WT lungs (p<0.01 by Fisher's exact test). To investigate the mechanism of enhanced tumorigenesis in IKKβ^{Δmye} mice, we performed immunohistochemistry for markers of proliferation (PCNA) and apoptosis (cleaved caspase-3). Although we did not observe any differences in cleaved caspase-3 staining between IKKβ^{Δmye} and WT lungs, there were significantly more PCNA$^+$ lung epithelial cells in IKKβ^{Δmye} mice compared to WT mice (**Figure 10E-F and data not shown**). To corroborate our findings from the urethane model, we utilized the LSL-Kras^{G12D} (Kras) lung tumor model (182). We performed bone marrow transplantation in Kras mice using either WT (WT→Kras) or IKKβ^{Δmye} (IKKβ^{Δmye}→Kras) donors. Lung tumors were induced in these bone marrow chimeras by IT injection of adenoviral vectors expressing Cre recombinase (adeno-Cre). Similar to urethane-injected IKKβ^{Δmye} mice, IKKβ^{Δmye}→Kras mice developed twice as many lung tumors as WT→Kras mice at 8 weeks after adeno-Cre treatment (**Figure 10G-H**). Together, these studies show that blocking NF-κB signaling in myeloid cells promotes lung tumorigenesis is both chemical and genetic models of lung cancer.
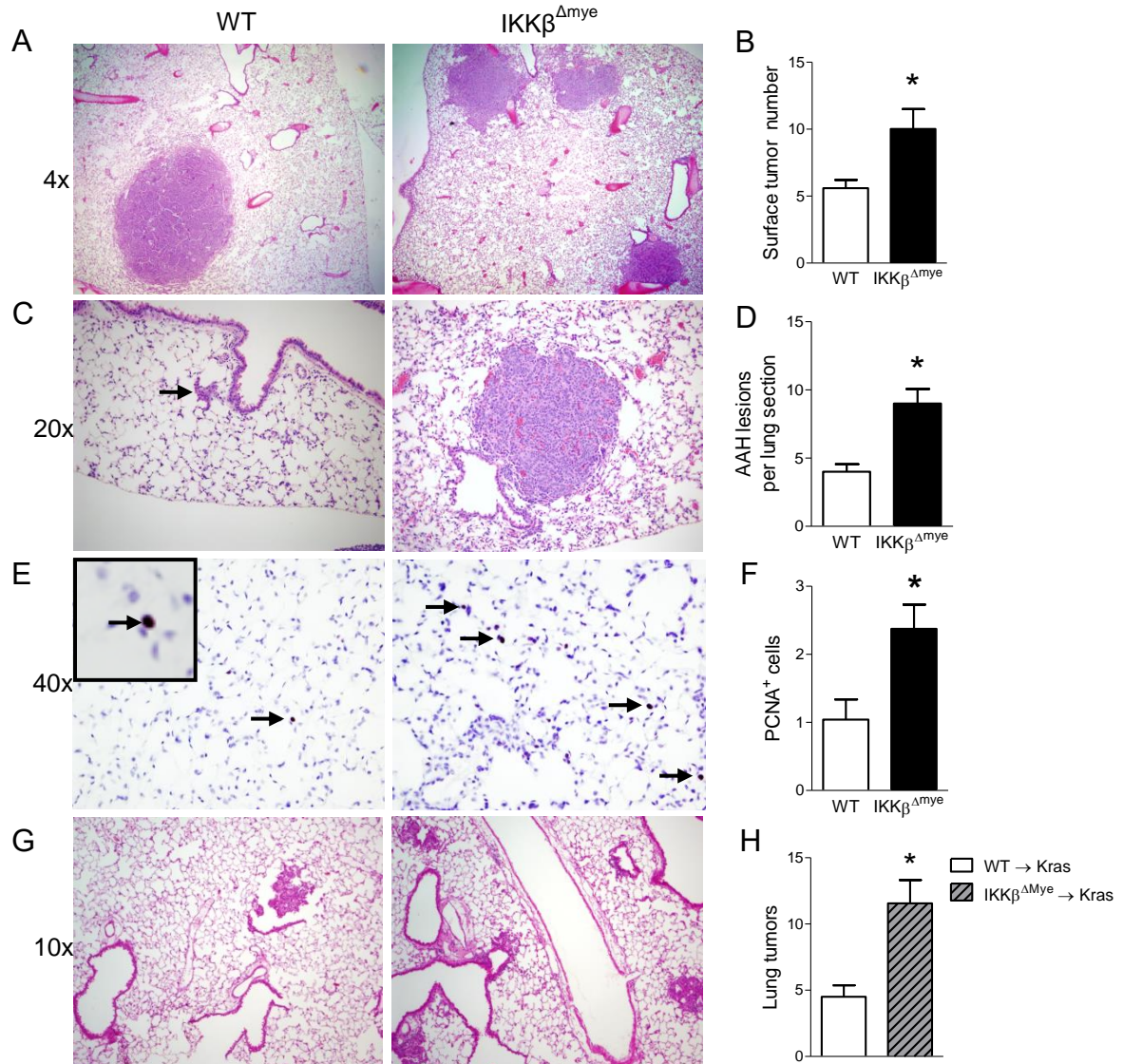
Figure 10: Inhibition of NF-κB signaling in myeloid cells increases lung tumorigenesis and epithelial cell proliferation.

A) Representative photomicrographs and B) Number of lung tumors in WT and IKKβ$^{\Delta mye}$ mice at 16 weeks after a single injection of urethane (n=16-22 mice per group). C) Representative photomicrographs showing an AAH lesion (red arrow) in the lung of WT mice or tumor in IKKβ$^{\Delta mye}$ mice, and D) Number of AAH lesions counted per H&E-stained lung section (3 sections per mouse) from WT and IKKβ$^{\Delta mye}$ mice harvested at week 6 after injection of urethane (n=9-10 mice per group). E) Immunostaining for PCNA$^+$ cells and (F) Number of PCNA$^+$ cells per lung section (averaged from 25 sequential fields taken at 40x magnification) from WT and IKKβ$^{\Delta mye}$ mice harvested at week 6 after urethane injection (n=3-4 per group). G-H) Lethally-irradiated LSL-Kras^{G12D} mice received bone marrow from WT (WT→Kras) or IKKβ$^{\Delta mye}$ (IKKβ$^{\Delta mye}$→Kras) mice. Lung tumors were induced by instillation of IT adeno-Cre (1.5x10^7 PFU). G) Representative photomicrographs and H) Number of lung tumors in WT→Kras and IKKβ$^{\Delta mye}$→Kras mice at 8 weeks after adeno-Cre (n=4-9 mice per group) *p < 0.05 by Student's t-test.

Since NF-κB is an important regulator of inflammation, we next investigated the role of myeloid NF-κB signaling on lung inflammation during tumorigenesis. No differences in inflammatory cells in BAL fluid were observed between untreated WT and IKKβ$^{\Delta mye}$ mice; however, at 6 weeks post-urethane injection, we observed increased inflammatory cells in BAL from IKKβ$^{\Delta mye}$ mice, indicating that heightened lung inflammation in IKKβ$^{\Delta mye}$ mice was an effect of carcinogen treatment (**Figure 11A**). To evaluate specific myeloid subpopulations, we performed flow cytometry on lung cells from IKKβ$^{\Delta mye}$ and WT mice (**Figure 11B**). Consistent with findings in BAL, no differences in neutrophil, monocyte, or macrophage cell populations were observed between untreated WT and IKKβ$^{\Delta mye}$ mice (**Figure 11C**). In contrast, we found elevated numbers of neutrophils in the lungs of IKKβ$^{\Delta mye}$ mice at 6 weeks post-urethane injection (**Figure 11D**). Additional studies in Kras model bone marrow chimeras showed similar findings with increased lung neutrophils in IKKβ$^{\Delta mye}$→Kras mice at 8 weeks after IT adeno-Cre injection compared to WT→Kras mice (**Figure 11E-F**).
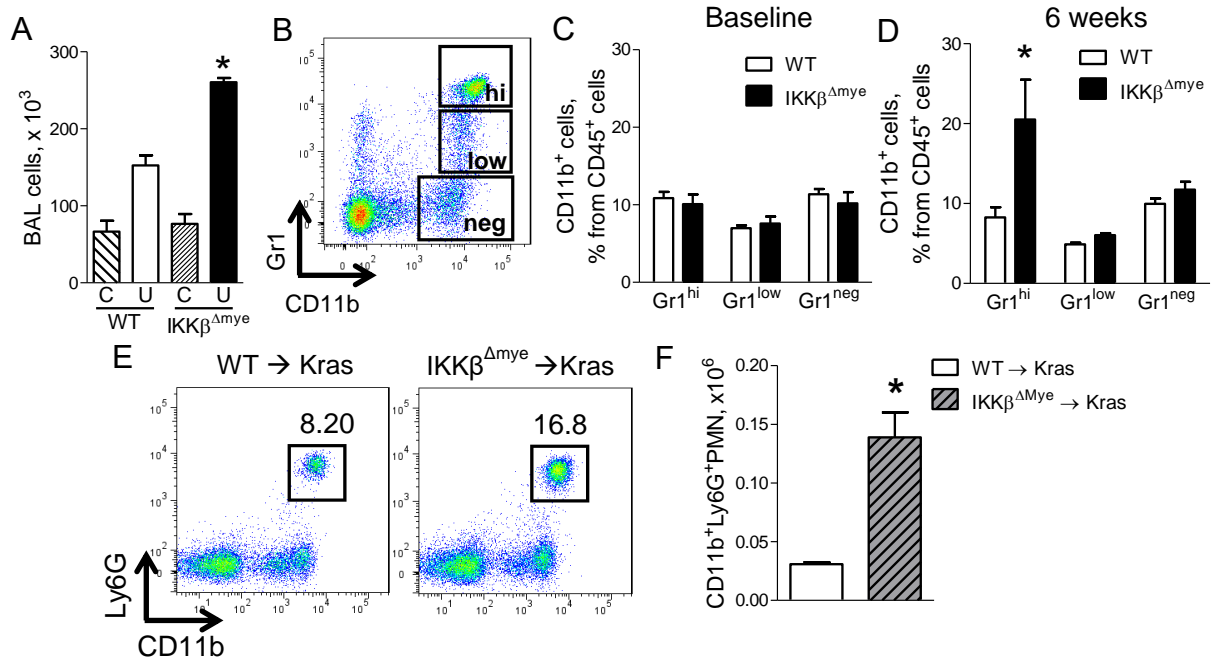
Figure 11: Neutrophils are increased in the lungs of mice lacking myeloid NF-κB signaling. A) Number of total BAL cells in WT and IKKβ^{Δmye} mice at baseline (C) and at 6 weeks after urethane injection (U) (n=7-9 mice per group; *$p < 0.05$ by one-way ANOVA compared with urethane-treated WT mice). B) Representative FACS plots and (C-D) Percentages of viable CD45$^+$/CD11b$^+$/Gr1^{hi} neutrophils (Gr1^{hi}), CD45$^+$/CD11b$^+$/Gr1^{low} monocytes (Gr1^{low}), and CD45$^+$/CD11b$^+$/Gr1^{neg} macrophages (Gr1^{neg}) in the lungs of WT and IKKβ^{Δmye} mice at (C) baseline and (D) 6 weeks after urethane injection (n=4-11 mice per group; *$p < 0.05$ by two-way ANOVA compared with WT). E) Representative FACS plots and (F) total viable CD45$^+$/CD11b$^+$/Ly6G$^+$ neutrophils in the lungs of WT→Kras and IKKβ^{Δmye}→Kras mice 8 weeks after adeno-Cre (n=4 mice per group; *$p < 0.05$ by Student's t-test compared with WT→Kras). Ly6G^{hi} identifies the granulocytic subgroup of the Gr1 marker.

In order to determine if neutrophils were important for lung carcinogenesis, we performed neutrophil depletion using antibodies against Ly6G (194). WT and IKKβ$^{\Delta mye}$ mice were injected with urethane and administered anti-Ly6G antibodies or isotype control IgG antibodies (100 μg) twice weekly for 6 weeks. A marked reduction in lung neutrophils was confirmed by flow cytometry (**Figure 12A-B**). While neutrophil depletion significantly reduced AAH lesions in lungs of IKKβ$^{\Delta mye}$ mice, we observed no effect of this treatment in WT mice (**Figure 12C**). Next, we tested the effect of early neutrophil depletion on lung tumor formation. A bone marrow transplantation study was incorporated into this experiment to verify that enhanced tumorigenesis in IKKβ$^{\Delta mye}$ mice was due to bone marrow-derived leukocytes in this model. Lethally-irradiated WT mice received bone marrow from IKKβ$^{\Delta mye}$ (IKKβ$^{\Delta mye}$→WT) or WT (WT→WT) donors. Bone marrow chimeras were injected with urethane and administered anti-Ly6G antibodies or isotype control IgG antibodies (100 μg) twice weekly for 6 weeks. At week 16 after urethane injection, we observed increased tumor formation in the lungs of control IgG-treated IKKβ$^{\Delta mye}$→WT mice compared to control (IgG-treated) WT→WT mice, indicating that enhanced tumorigenesis in IKKβ$^{\Delta mye}$ mice was due to bone marrow-derived cells. Neutrophil depletion in anti-Ly6G antibody-treated IKKβ$^{\Delta mye}$→WT mice reduced lung tumor numbers compared to IgG-treated IKKβ$^{\Delta mye}$→WT mice, identifying neutrophils as key players during early lung carcinogenesis (**Figure 12D**).
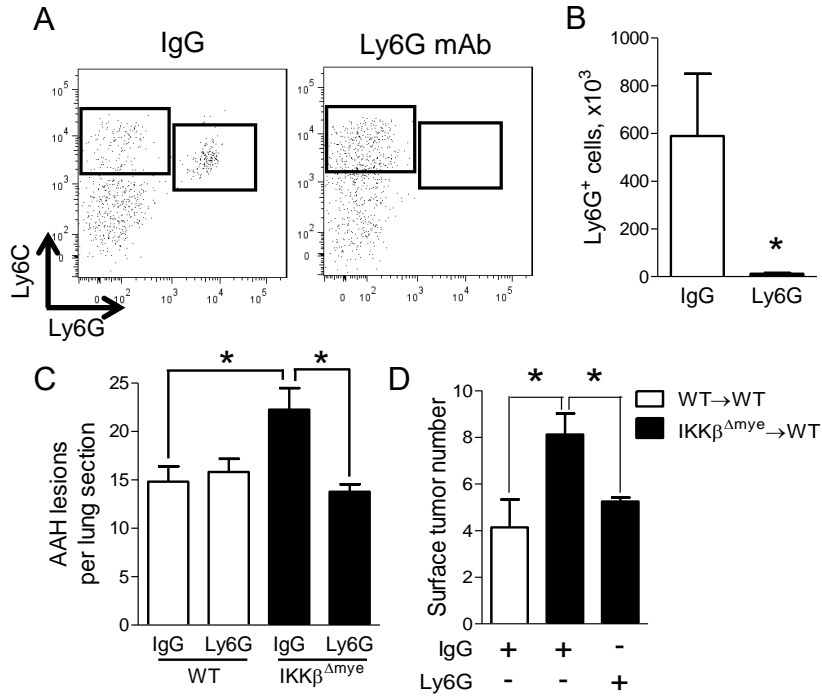
Figure 12: Neutrophils promote lung tumorigenesis in the absence of myeloid NF-κB signaling.

All mice were treated with isotype control IgG or anti-Ly6G depletion antibodies (100 µg by IP injection) for the first 6 weeks following urethane injection. A) Representative FACS plots and (B) total viable CD45$^+$/CD11b$^+$/Ly6C$^+$/Ly6G$^+$ lung neutrophils demonstrating depletion efficiency in IKKβ$^{\Delta mye}$ mice harvested 3 days after the last dose of antibody (n=4 mice per group; *p < 0.05 by Student's t-test). C) Number of AAH lesions per lung section from IgG- and anti-Ly6G-treated WT and IKKβ$^{\Delta mye}$ mice at 6 weeks after urethane injection (n=6-9 mice per group; *p < 0.05 by one-way ANOVA). D) Lethally-irradiated WT mice received bone marrow from WT or IKKβ$^{\Delta mye}$ mice. Lung tumors at 16 weeks after urethane injection in bone marrow chimera mice treated with IgG or anti-Ly6G antibodies for the first 6 weeks of tumorigenesis (n=6-8 mice per group; *p<0.05 by one-way ANOVA).

Myeloid-specific NF-κB inhibition results in increased IL-1β production by neutrophils following carcinogen exposure

To determine how IKKβ-deficient neutrophils exert their pro-tumorigenic effects during lung carcinogenesis, we characterized neutrophils from IKKβ^{Δmye} and WT mice according to morphological appearance, maturity, and function. We sorted CD45$^+$/CD11b$^+$/Ly6C$^+$/Ly6G$^+$ neutrophils (referred to below as Ly6G$^+$ cells), CD45$^+$/CD11b$^+$/Ly6C$^+$/Ly6G$^-$ monocytes, and CD45$^+$/CD11b$^+$/Ly6C$^-$/Ly6G$^-$ macrophages using fluorescence-activated cell sorting (FACS) from lungs of urethane-treated IKKβ^{Δmye} and WT mice. Morphometric analysis of these cells confirmed that Ly6G$^+$ cells had segmented nuclei, characteristic of mature neutrophils (**Figure 13A**). As early as 1 week post-urethane, IKKβ^{Δmye} mice had a nearly 3-fold increase in Ly6G$^+$ cells in the lungs compared to WT mice, while lung monocytes and macrophages, as well as peripheral blood neutrophils, were comparable between groups (**Figure 13B** and data not shown). To determine if loss of NF-κB signaling affected maturation of neutrophils, we measured expression of myeloperoxidase (MPO), an enzyme produced by mature neutrophils, in Ly6G$^+$ cells from IKKβ^{Δmye} and WT mice at 1 week after urethane injection (**Figure 13C**). Loss of NF-κB signaling in Ly6G$^+$ cells from IKKβ^{Δmye} mice did not impair MPO production (**Figure 13C-D**). We also examined N1/N2 markers in lung neutrophils by real-time PCR but did not observe differences in anti-tumorigenic N1 markers (TNFα, IL-12p35, ICAM1, IFNγ, iNOS) or pro-tumorigenic N2 markers (CCL2, CCL5, CCL17, VEGF, IL-10, Arg1) between neutrophils from urethane-injected WT and IKKβ^{Δmye} mice (**Figure 13E-F**). Since a subset of Ly6G$^+$ cells [granulocytic myeloid derived suppressor cells (MDSCs)] has been shown to promote tumorigenesis through suppression of anti-tumor responses from T lymphocytes (195), we assessed the ability of Ly6G$^+$ cells isolated from lungs of urethane-treated IKKβ^{Δmye} mice to suppress effector T (Teff) cell

proliferation in an allogeneic mixed lymphocyte reaction assay. As shown in **Figure 13G**, Ly6G$^+$ cells from IKKβ^{Δmye} mice failed to suppress proliferation of Teff cells stimulated by allogeneic dendritic cells, indicating that Ly6G$^+$ cells from IKKβ^{Δmye} mice do not act as MDSCs. These studies show that Ly6G$^+$ neutrophils from IKKβ^{Δmye} mice are mature cells that are not highly polarized towards N1 or N2 and do not exhibit immunosuppressive properties during early lung tumorigenesis.
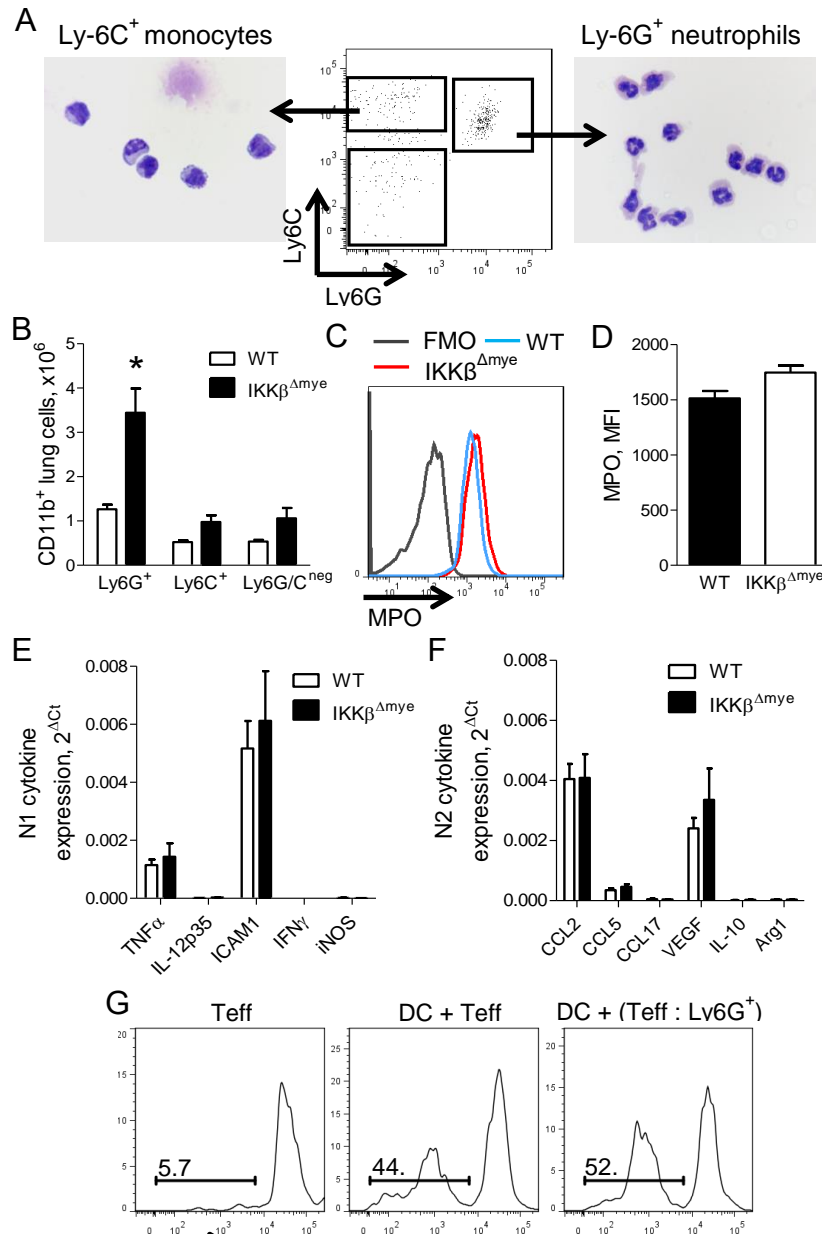
Figure 13: Mature neutrophils are increased in the lungs during early tumorigenesis in the absence of myeloid NF-κB signaling.
A) FACS sorting strategy and photomicrographs demonstrating cell morphology of lung monocytes (CD45+/CD11b+/Ly6C+/Ly6G-) and neutrophils (CD45+/CD11b+/Ly6C+/Ly6G+) isolated from lungs of WT and IKKβ$^{\Delta mye}$ mice at 1 week after urethane injection. B) Numbers of CD11b+/Ly6G+ neutrophils (Ly6G+), CD11b+/Ly6C+ monocytes (Ly6C+), and CD11b+/Ly6G^{neg}/Ly6C^{neg} macrophages (Ly6G/C^{neg}) in the lungs of WT and IKKβ$^{\Delta mye}$ mice at 1 week after urethane injection (n=3 mice per group, representative of 2 independent experiments; *$p < 0.05$ compared to WT by two-way ANOVA). C) Flow cytometry plot (including fluorescence minus one [FMO] control) and (D) mean fluorescence intensity (MFI) showing expression of MPO in viable CD45+/CD11b+/Ly6G+ cells from lungs of WT and IKKβ$^{\Delta mye}$ mice at 1 week after urethane injection (n=4 mice per group). Expression of (E) N1 and (F) N2 markers in CD45+/CD11b+/Ly6G+ cells isolated from lungs of IKKβ$^{\Delta mye}$ mice at 1 week after urethane injection (n=4-5 mice per group). G) CD45+/CD11b+/Ly6G+ cells isolated from lungs of IKKβ$^{\Delta mye}$ mice at 1 week after urethane injection do not impair the ability of allogeneic dendritic cells (DC) to induce proliferation of CFSE-labeled responder CD4+/CD25- T cells (Teff) (1:1, performed in duplicate).

Since we did not identify differences in maturation or function of neutrophils from IKKβ$^{\Delta mye}$ mice, we investigated whether differential production of inflammatory mediators could be responsible for increased tumorigenesis in the context of NF-κB inhibition. We measured mRNA and protein expression of a panel of cytokines (G-CSF, GM-CSF, IFNγ, IL-1β, IL-4, IL-6, IL-10, IL-12p40, KC, CCL2, and CCL3) in the lungs of IKKβ$^{\Delta mye}$ and WT mice at 1 week after urethane injection. Both KC mRNA and protein were increased in lungs of IKKβ$^{\Delta mye}$ mice, while IL-1β protein, but not mRNA, was upregulated (**Figure 14A-B**). For IL-1β, increased protein without increased mRNA expression suggests increased pro-IL-1β processing, which has previously been shown to occur in the setting of NF-κB inhibition (191). No differences in IL-1β protein levels were detected between untreated WT and IKKβ$^{\Delta mye}$ mice (**data not shown**). To determine the cellular source for increased IL-1β protein in IKKβ$^{\Delta mye}$ mice, we sorted myeloid cells from lungs at 1 week after urethane injection and measured IL-1β in conditioned media. Neutrophils from IKKβ$^{\Delta mye}$ mice secreted nearly twice as much IL-1β as monocytes or macrophages (**Figure 14C**) and produced more IL-1β than lung neutrophils from urethane-injected WT mice (**Figure 14D**), identifying IKKβ-deficient neutrophils as the source of increased IL-1β protein levels in the lungs. To verify that neutrophils were the primary source of IL-1β, we performed macrophage and neutrophil depletion studies in urethane-treated IKKβ$^{\Delta mye}$ mice. For macrophage depletion, urethane-treated IKKβ$^{\Delta mye}$ mice were administered liposomal clodronate or vehicle (liposomal PBS) by IT injection (186) and harvested at 1 week after urethane. Macrophage depletion did not alter IL-1β protein in the lungs of IKKβ$^{\Delta mye}$ mice (**Figure 14E**). For neutrophil depletion, urethane-treated IKKβ$^{\Delta mye}$ mice received IP injections of 100 μg of anti-Ly6G or isotype control IgG antibodies (130, 196) and lungs were harvested 1 week later. Neutrophil depletion was confirmed by flow cytometry, showing a reduction in the percentage of Ly6G^{+} cells within the CD45^{+}/CD11b^{+} gate from 45.2±2.9% in mice treated with control IgG antibodies to

48

1.0±0.6% in mice treated with anti-Ly6G antibodies (p<0.0001). Compared to IKKβ^{Δmye} mice treated with control IgG antibodies, anti-Ly6G antibody treatment significantly reduced IL-1β in the lungs (**Figure 14F**). Taken together, these studies point to IL-1β as a neutrophil-derived mediator that could support enhanced lung tumorigenesis.

Serine proteases have been implicated in the regulation of IL-1β processing by neutrophils (191); therefore, we performed inhibitor studies to determine the mechanism of dysregulated IL-1β release by lung neutrophils from IKKβ^{Δmye} mice. Lung neutrophils were isolated from urethane-treated WT and IKKβ^{Δmye} mice and cultured in the presence of inhibitors of caspase-1 (Ac-YVAD-cmk; YVAD), neutrophil elastase and proteinase 3 (MeOSuc-APPV-CMK; MeO), or cathepsin G (Z-GLP-CMK; GLP). While caspase-1 inhibition partially reduced IL-1β release from IKKβ^{Δmye} neutrophils, inhibition of the serine protease cathepsin G blocked nearly all IL-1β secretion from neutrophils of both WT and IKKβ^{Δmye} mice (**Figure 14G**). Additionally, gene expression of cathepsin G was upregulated in lung neutrophils from urethane-treated IKKβ^{Δmye} mice compared to WT mice, while no differences in expression were observed in caspase-1, neutrophil elastase, or proteinase 3 (**Figure 14H and data not shown**). These data implicate cathepsin G as the primary regulator of IL-1β processing by lung neutrophils in urethane-treated mice.
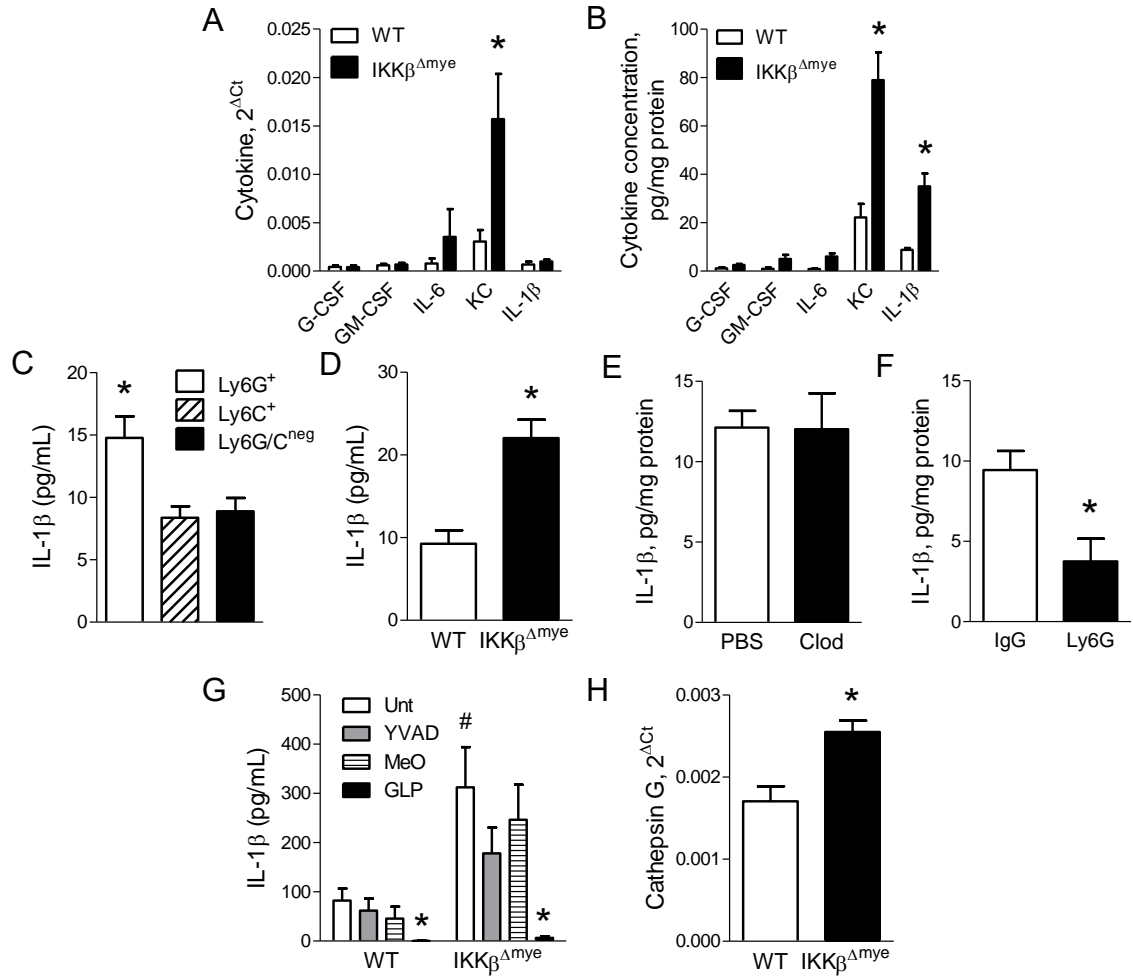
Figure 14: Neutrophils from IKKβ$^{\Delta mye}$ mice produce increased IL-1β following urethane injection.

Expression of cytokines by A) mRNA and B) protein in the lungs of WT and IKKβ$^{\Delta mye}$ mice harvested 1 week after urethane (n=10-11 mice per group; *p < 0.05 compared with WT by Student's t-test). C) Concentration of IL-1β in the conditioned media following 12-hour culture of lung Ly6G$^+$ neutrophils, Ly6C$^+$ monocytes, or Ly6G/C^{neg} macrophages isolated from IKKβ$^{\Delta mye}$ mice at 1 week after urethane injection (n=3; *p < 0.05 by one-way ANOVA compared with Ly6C$^+$ and Ly6G/C^{neg}). D) Concentration of IL-1β in the conditioned media following 12-hour culture of lung Ly6G$^+$ neutrophils from WT and IKKβ$^{\Delta mye}$ mice at 1 week after urethane injection (n=8 mice per group; *p < 0.05 by Student's t-test). E) IL-1β protein levels in lung homogenates at 1 week after urethane in the lungs of IKKβ$^{\Delta mye}$ mice treated with liposomal clodronate or PBS on day 5 following urethane injection (n=6 mice per group). F) IL-1β protein levels at 1 week after urethane in the lungs of IKKβ$^{\Delta mye}$ mice treated with anti-Ly6G antibodies (100 µg) or control IgG antibodies by IP injection on days -1, 2, and 5 relative to the day of urethane injection (n=3-5 mice per group; *p < 0.05 *p < 0.05 by Student's t-test compared with IKKβ$^{\Delta mye}$ mice treated with control IgG antibodies). Lung Ly6G$^+$ neutrophils were isolated from WT and IKKβ$^{\Delta mye}$ mice at 1 week after urethane injection. G) IL-1β concentration in the conditioned media after culture with inhibitors (all 100 µM) of caspase-1 (Ac-YVAD-CMK), neutrophil elastase and proteinase-3 (MeOSuc-APPV-CMK), or cathepsin G (Z-GLP-CMK) (n=3-8 replicates per group; #p>0.05 compared to WT Unt; *p<0.05 by two-way ANOVA compared to either WT or IKKβ$^{\Delta mye}$ Unt). H) mRNA expression of cathepsin G in lung Ly6G$^+$ neutrophils isolated from WT and IKKβ$^{\Delta mye}$ mice at 1 week after urethane injection (n=5 mice per group; *p < 0.05 by Student's t-test)

Systemic NF-κB inhibition increases IL-1β production in mice and humans with lung cancer

We next sought to determine whether IL-1β dysregulation could be detected following treatment with pharmacological NF-κB inhibitors in mice and human NSCLC patients. WT mice were treated with the proteasome inhibitor bortezomib (1 mg/kg) (109, 110) or vehicle by IP injection on days 2 and 6 following urethane injection and harvested at day 7 (**Figure 15A**). We observed elevated numbers of neutrophils in BAL from bortezomib-treated mice compared to vehicle-treated controls (**Figure 15B**). In addition, we found increased IL-1β protein in both serum and lungs of bortezomib-treated mice compared to mice treated with vehicle (**Figure 15C-D**). To test whether these effects were common to different classes of NF-κB inhibitors, we repeated our studies using BAY 11-7082 (BAY). NF-κB inhibition was verified by luciferase activity as a measure of NF-κB activity in vehicle- or BAY-treated NF-κB reporter mice (184) after urethane injection (**Figure 16**). At 1 week after urethane injection, BAY treatment resulted in increased neutrophils in BAL and lung tissue (**Figure 15E-G**). BAY-treated mice also had elevated IL-1β protein in lung homogenates compared to vehicle-treated mice, similar to IKKβ$^{\Delta mye}$ mice (**Figure 15H**). Unlike IKKβ$^{\Delta mye}$ mice, however, KC expression was not increased in BAY-treated WT mice (**Figure 17**).
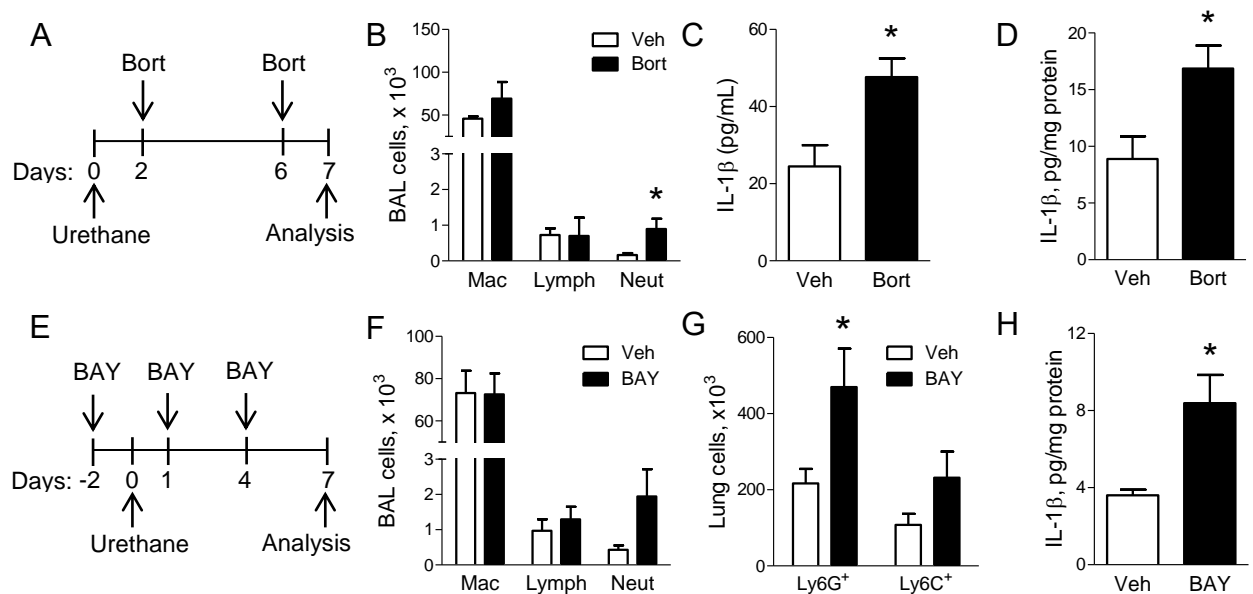
Figure 15: Pharmacological inhibition of NF-κB increases IL-1β in mice.
A) Schematic representation of NF-κB inhibition protocol using bortezomib (Bort). In addition to urethane, WT mice were treated with IP injections of Bort (1 mg/kg) or vehicle control (Veh). B) BAL cells in Bort- or Veh-treated WT mice at 1 week after urethane injection (n=4-5 mice per group; *p<0.05 by Student's t-test compared to Veh). C) Serum and (D) lung IL-1β protein levels from Bort- or Veh-treated WT mice 1 week after urethane (n=6 mice per group; *p<0.05 by Student's t-test compared to Veh). E) Schematic representation of the NF-κB inhibition protocol using BAY 11-7082 (BAY). In addition to urethane, WT mice were treated with IP injections of the specific NF-κB inhibitor BAY (10 mg/kg) or Veh. F) BAL cells in BAY- and Veh-treated WT mice at 1 week after urethane injection (n=8 mice per group). G) Number of Ly6G+ neutrophils and Ly6C+ monocytes in the lungs of BAY- or Veh-treated mice at 1 week after urethane injection (n=4-5 mice per group; *p<0.05 by Student's t-test compared to Veh). H) IL-1β protein levels in the lungs of BAY- or Veh-treated mice at 1 week after urethane injection (n=8 mice per group; *p<0.05 by Student's t-test compared to Veh).
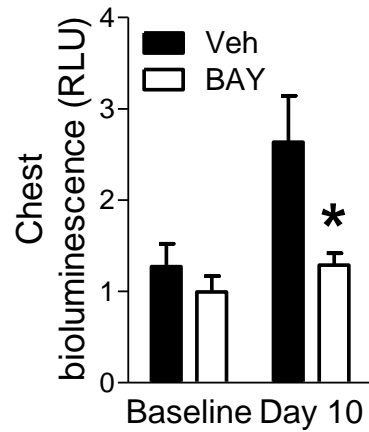
Figure 16: BAY 11-7082 treatment blocks NF-κB activation in reporter mice.
NF-κB reporter mice were injected with a single dose of urethane and treated with BAY 11-7082 (10 mg/kg by IP injection) or vehicle control 3 times per week. Chest bioluminescence was measured at baseline (prior to urethane treatment) and 10 days after urethane injection (RLU = relative light units). NF-κB reporter mice that express a green fluorescent protein-luciferase fusion protein under control of an NF-κB dependent promoter were injected intravenously with D-luciferin (1 mg) followed by bioluminescent imaging (n=3-5 mice per group; *p<0.05 by Student's t-test compared to Veh).
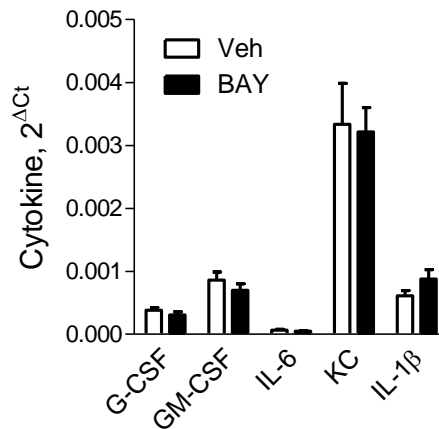
Figure 17: KC expression is not increased upon systemic NF-κB inhibition in WT mice.
Expression of cytokines by mRNA in the lungs of IKKβ$^{\Delta mye}$ mice injected with urethane and treated with BAY 11-7082 (10 mg/kg) or vehicle control (Veh) for 1 week (n=8 mice per group).

To investigate the relevance of our mouse model findings to human NSCLC, we obtained blood samples from a completed study involving 28 chemotherapy-naïve individuals with advanced stage (III-IV) NSCLC (protocol NCT01633645) (**Table 2**). In this study, patients received one cycle of bortezomib followed by a standard chemotherapy/bortezomib combination regimen. In plasma obtained before and 24 hours after the first dose of bortezomib (1 mg/m^2), we measured a panel of cytokines (IL-1β, IL-8, TNF, and IL-6) using cytometric bead array and found that treatment with bortezomib significantly increased IL-1β protein in the plasma of advanced NSCLC patients; however, no differences were detected in IL-8, TNF, or IL-6 (**Figure 18A-D**). In addition, we found that after controlling for age and performance status, IL-1β level at baseline significantly correlated with reduced progression-free survival in this cohort (p=0.026) (**Figure 18E**).

Patient Characteristics	Total (n=28)
Age, y	75.5 (68.5, 79.2)*
Male gender	22 (78.6%)†
Cancer stage	
IIIB	1 (3.6%)†
IV	27 (96.4%)†
Cancer histology	
Adenocarcinoma	11 (39.3%)†
Squamous	11 (39.3%)†
Other NSCLC	6 (21.4%)†
Performance score	
0	19 (67.9%)†
1	9 (32.1%)†
Progression-free survival, mo	3.6 (1.7, 6.4)*
Overall survival, mo	10.2 (4.7, 21.0)*

Table 2: Characteristics of NSCLC patients treated with bortezomib.
*   Data are represented as median (interquartile range)
†   Data are represented as total (percent)
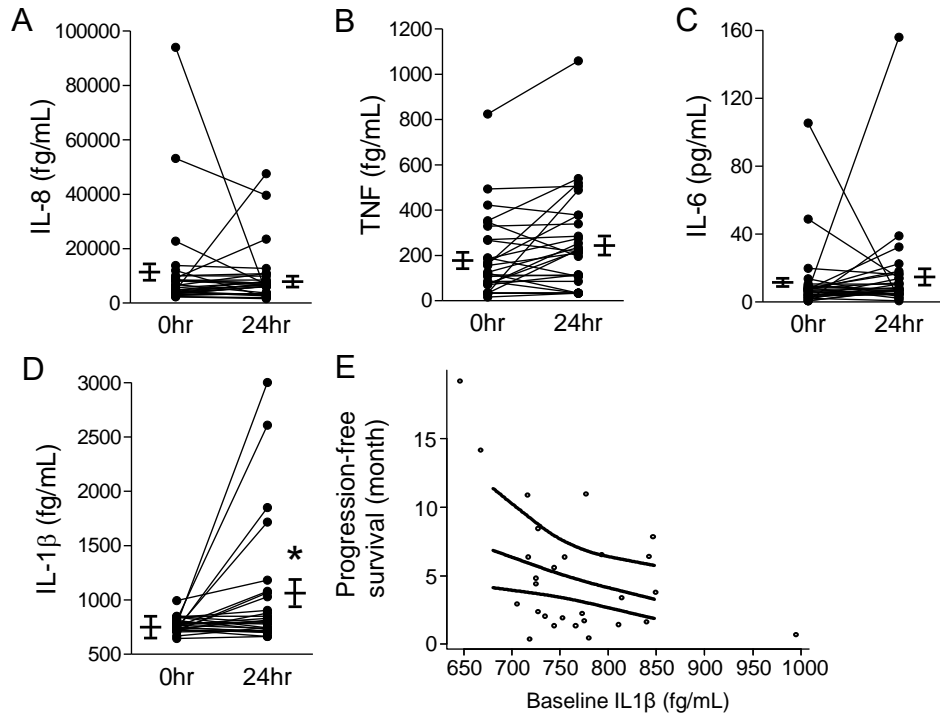
Figure 18: Bortezomib treatment increases plasma IL-1β and indicates worse survival in NSCLC patients.

A) IL-8, (B) TNF, (C) IL-6, and (D) IL-1β protein levels in the plasma of NSCLC patients treated before (0hr) and 24hr after treatment with bortezomib (1 mg/m^2) (n=28 patients; *p < 0.05 by Student's t-test compared with 0 hr). E) Correlation analysis between progression-free survival and baseline plasma IL-1β protein levels in advanced NSCLC patients treated with bortezomib plus standard chemotherapy (p=0.026 by adjusted Spearman's correlation).

IL-1β promotes lung tumorigenesis, enhances epithelial cell proliferation, and mediates resistance to NF-κB inhibitor therapy

Since IL-1β production is increased in tumor models in the setting of myeloid and systemic NF-κB inhibition, we investigated the impact of IL-1β on lung tumorigenesis using the clinically available IL-1 receptor antagonist (IL-1ra, anakinra/Kineret®). IL-1ra (60 mg/kg/day) was delivered during the first 4 weeks after urethane injection to WT and IKKβ^{Δmye} mice using subcutaneously implanted osmotic pumps (**Figure 19A**). Osmotic pumps filled with PBS were used as controls. Effective drug delivery was indicated by reduced BAL neutrophils as well as reduced expression of IL-1 signaling targets KC, CXCL5, and IL-1β in the lungs at 1 week after urethane injection (**Figure 19B-C**). As shown in **Figure 19D**, IL-1ra treatment significantly decreased the number of AAH lesions in the lungs of IKKβ^{Δmye} mice at 6 weeks after urethane injection. To evaluate the impact of IL-1β signaling on tumor formation, we repeated these studies and harvested mice 16 weeks after urethane treatment. We found that IL-1ra treatment reduced lung tumors in IKKβ^{Δmye} mice by more than 50% compared to IKKβ^{Δmye} mice treated with PBS control (**Figure 19E**). Based on our finding that IKKβ^{Δmye} mice have increased lung epithelial cell proliferation during tumorigenesis (**Figure 10E-F**), we tested whether IL-1β could exert its pro-tumorigenic effects by altering proliferation of epithelial cells. We performed PCNA immunostaining on lung sections from IL-1ra- and PBS-treated IKKβ^{Δmye} mice harvested 6 weeks after urethane and found reduced PCNA$^+$ lung epithelial cells in IL-1ra-treated IKKβ^{Δmye} mice (**Figure 19F**), demonstrating that IL-1β signaling supports epithelial cell proliferation during tumorigenesis. Together, these results indicate a pro-tumorigenic role for IL-1β in the setting of NF-κB inhibition in myeloid cells.
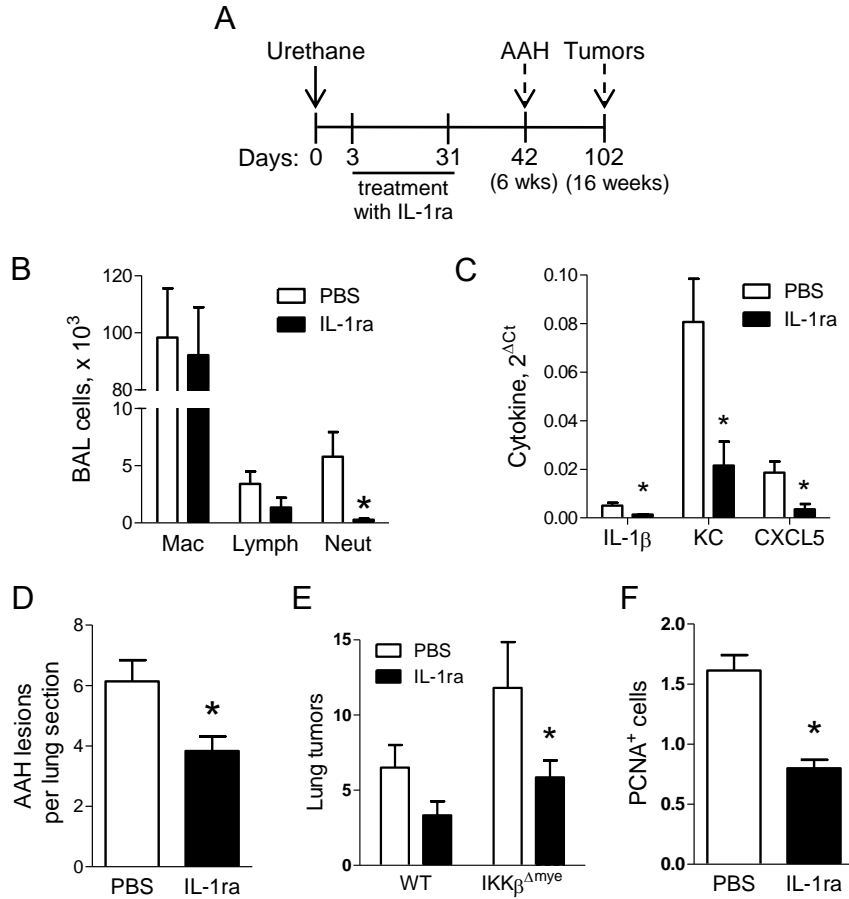
Figure 19: IL-1β facilitates lung tumorigenesis by stimulating epithelial cell proliferation

A) Schematic representation of IL-1 receptor antagonist (IL-1ra) treatment protocol. WT and IKKβ^{Δmye} mice were injected with a single dose of urethane and treated by osmotic pump delivery of 60 mg/kg/day of IL-1ra or PBS for the first 4 weeks. B) Total BAL cells and (C) mRNA expression of cytokines in the lungs of urethane-injected IKKβ^{Δmye} mice treated with IL-1ra or PBS for 1 week (n=4-5 mice per group; *p<0.05 by Student's t-test compared to PBS). D) Number of AAH lesions per H&E-stained lung section harvested from IKKβ^{Δmye} mice at week 6 after injection of urethane (n=9 mice per group, *p<0.05 by Student's t-test compared with PBS). E) Lung tumors on H&E-stained lung sections from WT and IKKβ^{Δmye} mice cut at predetermined depths (5 sections per mouse, n=7 mice per group; *p<0.05 by one-way ANOVA compared with PBS-treated IKKβ^{Δmye} mice). F) Number of PCNA$^+$ cells per lung section (averaged from 25 sequential fields taken at 40x magnification) from IKKβ^{Δmye} mice harvested at week 6 after urethane injection (n=9 mice per group; *p<0.05 by Student's t-test compared with PBS).

Since IL-1β is dysregulated and supports tumor cell proliferation in the context of NF-κB inhibition, we next tested whether the addition of IL-1ra could improve the efficacy of NF-κB inhibitor therapy in two different lung cancer models. In the first model, we injected murine Lewis lung carcinoma (LLC) cells subcutaneously into the flanks of syngeneic WT mice. When tumors reached 1 cm in diameter, mice were divided into four treatment groups: bortezomib, IL-1ra, bortezomib plus IL-1ra, or vehicle control. Bortezomib (or vehicle) was administered by IP injection twice weekly, and IL-1ra (or PBS control) was administered throughout the treatment course via osmotic pump. Whereas monotherapy with bortezomib or IL-1ra did not affect tumor growth, combination therapy with bortezomib and IL-1ra significantly reduced tumor growth compared with all other groups at day 10 after initiating treatment (**Figure 20**).
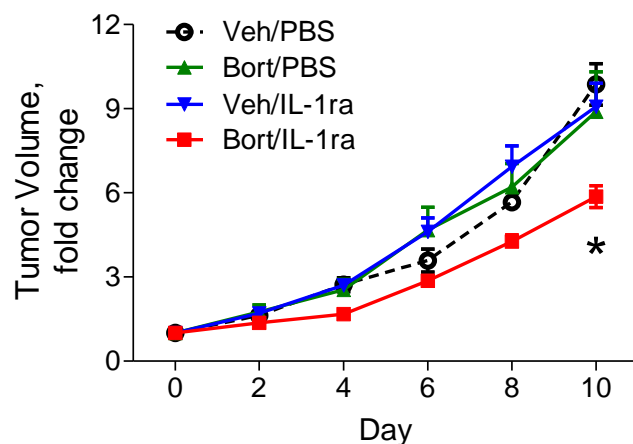
Figure 20: Combination therapy with bortezomib and IL-1ra slows tumor growth.
Fold change of subcutaneous LLC tumor volume over 10 days of treatment with vehicle control, bortezomib, IL-1ra, or bortezomib plus IL-1ra (n=6-9 mice per group; *p<0.05 by one-way ANOVA compared with control).

For the second model, we used doxycycline (dox)-inducible Kras^{G12D} mice (183). In a preliminary study, we treated mice with dox for 4 weeks followed by bortezomib twice weekly for 1 week and found increased neutrophils in the lungs compared to vehicle-treated mice (**Figure 21A**). Subsequently, we treated inducible Kras^{G12D} mice with dox for 4 weeks and then randomized mice to treatment with bortezomib, IL-1ra, bortezomib plus IL-1ra, or vehicle control for 4 additional weeks. While treatment with bortezomib reduced tumor numbers compared to vehicle control and IL-1ra groups, lung tumors were reduced by 90% in mice administered combination therapy with bortezomib and IL-1ra (**Figure 21B-C**). Collectively, our findings indicate that combination therapy with bortezomib and IL-1ra reduced tumor formation and growth, and was more effective than bortezomib alone.
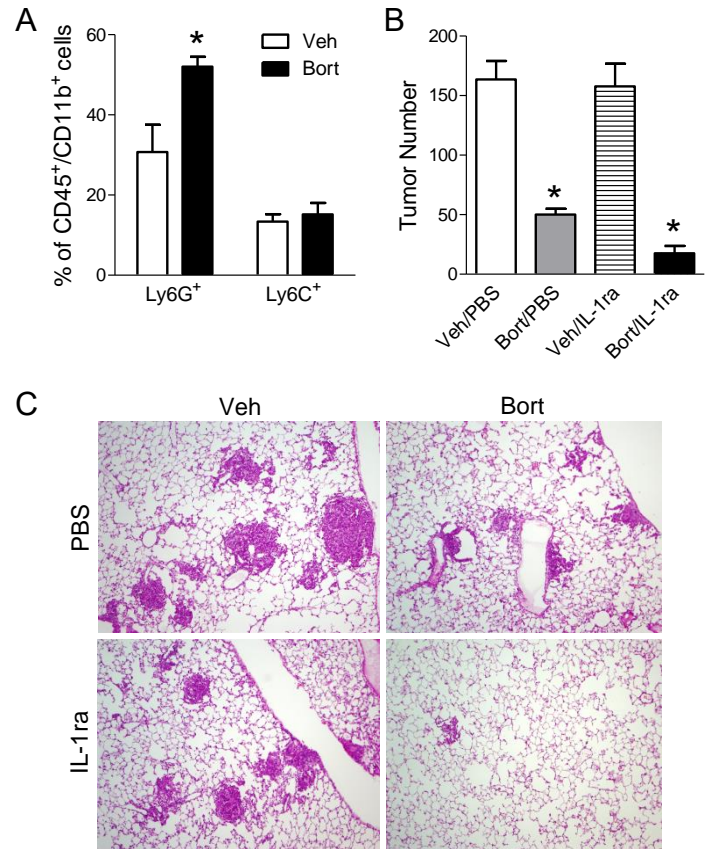
Figure 21: Combination therapy with bortezomib and IL-1ra reduces tumor number in Kras^{G12D} mice.

A-C) Inducible Kras^{G12D} mice were treated with doxycycline (dox) for 4 weeks to develop lung tumors. (A) Percentage of Ly6G$^+$ and Ly6C$^+$ cells in the lungs of dox-inducible Kras^{G12D} mice treated for 1 additional week with Bort or Veh plus dox (*p<0.05 by Student's t-test compared to Veh). (B) Numbers of surface lung tumors and (C) Representative photomicrographs of lung tumors in mice treated with dox alone for 4 weeks followed by 4 weeks of treatment with dox plus vehicle control, bortezomib, IL-1ra, or bortezomib plus IL-1ra (n=6-7 mice per group; *p<0.05 by one-way ANOVA compared with control.

Discussion

Our studies identify IL-1β as a targetable, pro-tumorigenic mediator that contributes to resistance of lung tumors to NF-κB inhibitors. We showed that inhibition of NF-κB in myeloid cells enhances lung tumorigenesis and paradoxically increases infiltration of neutrophils into the lungs. NF-κB-deficient neutrophils produced elevated levels of IL-1β, which was regulated by the serine protease cathepsin G. Consistent with studies in mice with myeloid-specific NF-κB inhibition, systemic delivery of pharmacological NF-κB inhibitors to WT mice significantly increased lung neutrophils and IL-1β production during lung tumorigenesis. In humans with advanced stage NSCLC, plasma IL-1β concentration inversely correlated with progression-free survival and IL-1β levels were increased following treatment with the proteasome inhibitor bortezomib. Neutrophil depletion studies and pharmacological IL-1ra treatment, both of which reduced lung tumors in the setting of myeloid NF-κB inhibition, support a causative role for neutrophil-derived IL-1β in lung tumorigenesis. Further, we demonstrated that combined treatment with bortezomib and IL-1ra reduces tumor formation and growth *in vivo* and that IL-1β exerts its pro-tumorigenic effects by stimulating lung epithelial cell proliferation. In addition to demonstrating an important role for IL-1β in promoting lung carcinogenesis and mediating resistance to NF-κB inhibitors, these data provide support for use of rational combined biological therapies to treat lung cancer.

Together with existing literature, our findings suggest that the lung microenvironment could support both pro- and anti-tumorigenic outcomes resulting from inhibition of NF-κB signaling. Consistent with our previous studies showing pro-tumorigenic outcomes from long-term bortezomib treatment (110), these data demonstrate that inhibition of NF-κB signaling specifically in myeloid cells enhances lung tumorigenesis. Our findings are also in agreement with a recent report in which myeloid

NF-κB inhibition supported enhanced growth of melanomas (179). In opposition, previous studies using a colon cancer model and a model of lung cancer induced by oncogenic *Kras* plus cigarette smoke found that inhibition of NF-κB signaling in myeloid cells inhibited tumorigenesis (Greten et al., 2004; Takahashi et al., 2010). We suggest that differences in tumorigenic outcomes in response to myeloid-specific NF-κB inhibition may be due to differential effects on pre-existing inflammation in the tumor microenvironment. Both the azoxymethane plus dextran sulfate colon cancer model and the oncogenic *Kras* plus cigarette smoke model are highly inflammatory models in which myeloid NF-κB inhibition reduces carcinogenesis as well as cytokine expression and inflammatory cell infiltration (Greten et al., 2004; Takahashi et al., 2010). In contrast, the lung cancer models in our studies result in only mild inflammation, and myeloid NF-κB inhibition increases inflammation in these settings. Therefore, it may be that the overall impact of myeloid NF-κB inhibition on tumorigenesis is dependent upon the inflammatory environment. In environments with high levels of pre-existing inflammation, inhibition of NF-κB signaling may reduce pro-tumorigenic inflammation by blocking transcription of NF-κB-dependent mediators, consequently suppressing tumor formation and growth. In contrast, up-regulation of IL-1β processing by neutrophils may play an important pro-tumorigenic role in less inflammatory environments, which may be more similar to human lung cancer, by providing important proliferation signals to mutated epithelial cells. In either case, it may be that combination biological approaches to block inflammatory signaling are superior to NF-κB inhibition alone.

In our studies, we discovered that neutrophils play critical roles during early lung tumor formation. We show that both myeloid-specific and systemic inhibition of NF-κB induces an increase in lung neutrophils, potentially through increased recruitment or prolonged cell survival, which has been previously described for NF-κB-inhibited neutrophils (197, 198). Depletion of neutrophils during early tumor initiation and promotion

stages reduced lung tumor formation in our model, consistent with previous reports using oncogenic *Kras* models, which showed reduced tumorigenesis with neutrophil depletion or genetic neutrophil elastase deficiency (199, 200). The N1/N2 neutrophil polarization paradigm has been used to explain anti- or pro-tumorigenic functions of neutrophils (130). Several studies have shown that N2 tumor-associated neutrophils exert their pro-tumorigenic properties through production of angiogenic factors, matrix-degrading enzymes, and immunosuppression (Reviewed in Sionov et al., 2014). In contrast, our studies show that neutrophils with inhibited NF-κB signaling are not highly polarized towards N1 or N2 and are not immunosuppressive. Instead, NF-κB-deficient neutrophils have a unique pro-tumorigenic phenotype characterized by dysregulated processing of the inflammatory mediator IL-1β.

While we identified an important role for neutrophils in accelerating lung tumorigenesis in the context of NF-κB inhibition, other cell types may also contribute to this phenotype. Although not directly tested in our studies, interactions between neutrophils and macrophages may be important for creating a pro-tumorigenic environment in the lungs. This idea is supported by our previous finding that macrophages are important for urethane-induced tumorigenesis (186), as well as a recent study demonstrating that macrophages with inhibited NF-κB signaling are unable to mediate anti-tumor responses against metastatic melanoma cells (179). Future studies are necessary to fully elucidate interactions between inflammatory cell types and epithelial cells that regulate lung carcinogenesis.

A connection between elevated IL-1β and lung cancer in humans has been suggested by studies showing that a single nucleotide polymorphism (-31C-T) in *IL1B* increases IL-1β expression and lung cancer risk (201, 202). Our studies extend these findings by showing that IL-1β levels in plasma were inversely correlated with progression-free survival of NSCLC patients. Further, we found that plasma IL-1β levels of NSCLC

patients increase following NF-κB inhibition with the proteasome inhibitor bortezomib, suggesting that our explanation for resistance to NF-κB inhibitor therapy may be relevant to NSCLC patients.

We found that both myeloid-specific and systemic NF-κB inhibition increase IL-1β protein expression in the lungs. Although IL-1β mRNA expression is regulated by the NF-κB pathway (203), our findings are consistent with previous reports showing that NF-κB inhibition in myeloid cells increases IL-1β processing under conditions of septic shock and acute lung injury (191, 197, 204). While IL-1β processing in most cells is thought to be primarily regulated by the inflammasome, serine proteases have been implicated in IL-1β processing by neutrophils (191, 205). Our findings indicate that cathepsin G strongly regulates IL-1β production by neutrophils and that expression of cathepsin G is upregulated in neutrophils with inhibited NF-κB, potentially explaining the increased IL-1β production in this setting. Since cathepsin G has been correlated with tumor grade and clinical stage in NSCLC (206), future studies targeting this protease could be warranted.

Our studies demonstrate that the addition of IL-1 signaling blockade to NF-κB inhibitor therapy improves the effectiveness of NF-κB inhibition to reduce lung tumor formation and growth. In a heterotopic flank tumor model, combination therapy was the only regimen that slowed tumor growth compared to vehicle control. In the dox-inducible Kras^{G12D} model, bortezomib monotherapy reduced tumor formation but combination therapy with bortezomib and IL-1ra was most effective. These findings indicate that the effects of bortezomib are variable and model-dependent. In contrast, we consistently showed impressive responses to therapy with combination bortezomib/IL-1ra treatment. Of the 35 clinical trials included in the ClinicalTrials.gov database that investigate bortezomib in lung cancer, only three have used combined therapy with bortezomib and another targeted agent. Since combined targeted therapies may be the most direct way to manage disease and reduce nonspecific side effects from treatment (207), our studies

support future human studies combining NF-κB inhibitors with IL-1ra or other targeted

biological therapies aimed at overcoming resistance mechanisms.

CHAPTER IV: CONCLUDING REMARKS

Summary

Together with existing literature, the work presented in this dissertation identifies separate roles for NF-κB signaling in epithelial and myeloid cells during lung carcinogenesis. NF-κB signaling in epithelial cells has been shown to promote tumorigenesis in a variety of lung cancer models through increased epithelial cell proliferation and/or survival (83, 84, 86–88). NF-κB signaling in myeloid cells, on the other hand, seems to play different roles during tumorigenesis depending on the degree of inflammation present in the lung microenvironment. When lung inflammation is robust, blocking myeloid NF-κB signaling appears to be protective by reducing destructive inflammatory signaling (176). However, our studies show that in a less inflammatory environment, which is more closely related to the low-grade inflammation commonly associated with cancer, blocking NF-κB signaling in myeloid cells supports pro-tumorigenic inflammatory signaling. One important mechanism for tumor promotion in this context is dysregulation of IL-1β processing by neutrophils. The resulting elevated levels of mature IL-1β support tumorigenesis by increasing proliferation of epithelial cells. Combined inhibition of NF-κB and IL-1 signaling pathways impedes lung tumor formation and growth, representing the potential of combination therapies with NF-κB inhibitors and other agents for lung cancer treatment.

Additional data and future directions

Role of myeloid NF-κB signaling in lung tumor angiogenesis

In addition to discovering increased numbers of lung tumors in mice with myeloid cell-specific inhibition of NF-κB signaling, we also observed that the lung tumors in these mice were about half the size of those in WT mice at 16 weeks after urethane injection (**Figure 22A**). Since NF-κB is known to regulate angiogenesis, a process that is critical for continuous outgrowth of tumors (208–212), we performed immunostaining on lung sections for the endothelial cell marker CD34 to compare blood vessel density within tumors from WT and IKKβ$^{\Delta mye}$ mice harvested 16 weeks after urethane. Tumors from IKKβ$^{\Delta mye}$ mice contained significantly fewer blood vessels than those from WT mice (**Figure 22B-C**). Protein expression of vascular endothelial growth factor (VEGF), an NF-κB-regulated mediator of angiogenesis (213–215), was also reduced in the lungs of IKKβ$^{\Delta mye}$ mice (**Figure 22D**). Taken together, these data suggest that inhibition of NF-κB signaling in myeloid cells limits tumor size by reducing angiogenesis.
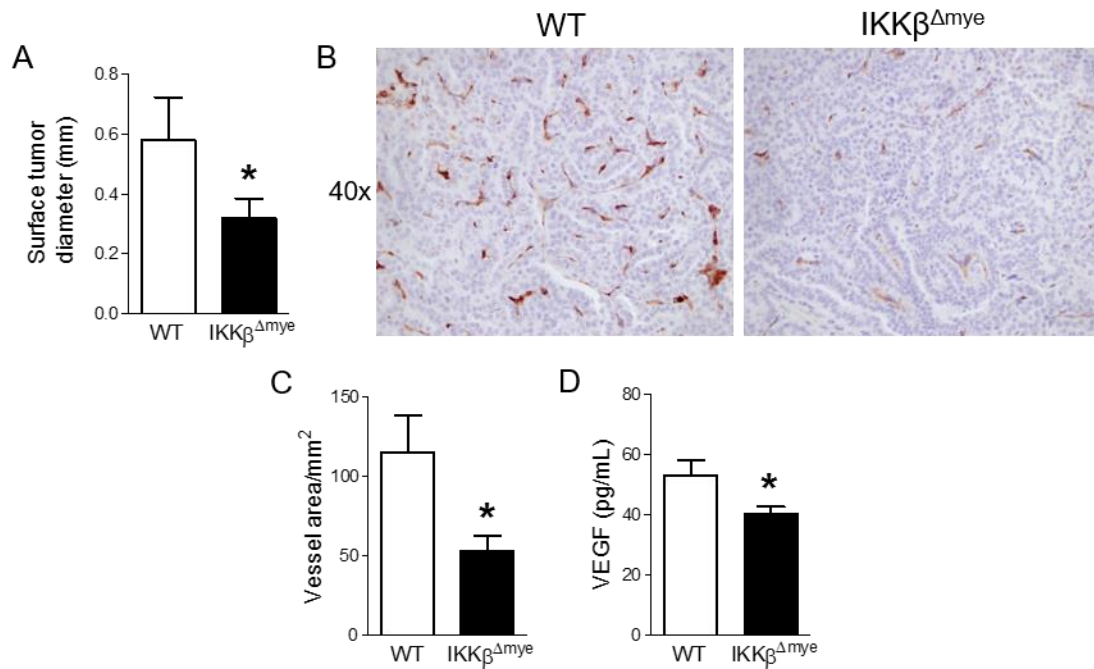
Figure 22: IKKβ$^{\Delta mye}$ mice have smaller lung tumors due to decreased angiogenesis. A) Diameters of surface lung tumors from WT and IKKβ$^{\Delta mye}$ mice at 16 weeks after urethane injection (n=16-22 mice per group). B) Representative photomicrographs of lung sections from tumor-bearing WT and IKKβ$^{\Delta mye}$ mice immunostained with antibodies against CD34. C) Blood vessel density in lung tumors from WT and IKKβ$^{\Delta mye}$ mice was calculated as the number of CD34^{+} endothelial cells per square millimeter of tumor area (n=5-7 mice per group). D) Concentration of VEGF protein in the BAL of WT and IKKβ$^{\Delta mye}$ mice harvested at 16 weeks after urethane injection (n=7-8 mice per group). *p<0.05 by Student's t-test compared to WT.

Previous studies have demonstrated roles for both macrophages and neutrophils in tumor angiogenesis. The presence of M2-like TAMs has been associated with increased tumor angiogenesis and poor patient prognosis in lung and other cancers (216–218). These TAMs support multiple steps required for angiogenesis, including degradation of the extracellular matrix as well as the migration and proliferation of endothelial cells (219). Our group has shown that depletion of macrophages during later stages of lung tumorigenesis suppresses tumor angiogenesis and decreases VEGF expression in the lung, identifying macrophages as a critical cell population for angiogenesis in lung tumor progression (186). Together with the current study, which shows a similar reduction in tumor vascularity and VEGF expression, these findings suggest that NF-κB signaling in macrophages and/or other myeloid cells supports the production of pro-angiogenic factors, as has been previously described for VEGF, MMP9, IL-1, TNFα, and FGF2 (215, 220–222). TANs have also been shown to play roles in tumor angiogenesis through MMP- and NE-mediated extracellular matrix degradation in models of hepatocellular carcinoma, chronic colitis-associated cancer, and pancreatic cancer (223–225). However, the role of TANs in lung tumor angiogenesis has not been determined. Studies comparing production of specific pro-angiogenic mediators from both WT and NF-κB-deficient TAMs and TANs may uncover different NF-κB-regulated mechanisms of tumor angiogenesis that can be targeted for cancer treatment.

Role of the inflammasome in lung tumorigenesis

Inflammasomes were first described in 2002 and have since become targets of interest for inflammatory conditions such as cryopyrin (NLRP3)-associated periodic syndrome, gout, diabetes, and, more recently, cancer (226, 227). Inflammasomes are a

group of molecular complexes comprised of a sensor/scaffolding protein (NLR), adaptor protein (ASC), and pro-caspase-1, which converts pro-IL-1β and pro-IL-18 to their processed, bioactive forms in response to various stimuli (228). Under non-cancerous conditions, activation of the inflammasome initiates an inflammatory cascade which results in immune cell recruitment for pathogen clearance. However, under cancerous conditions, inflammasomes can become constitutively active and contribute to metastasis, angiogenesis, and proliferation through IL-1β-mediated mechanisms (229).

To determine the role of inflammasomes in lung cancer, we investigated tumor formation in response to the lung carcinogen urethane in mice deficient in caspase-1 (Casp1 KO), the conserved enzymatic subunit of inflammasomes. Since Casp1 KO mice were on the tumor-resistant C57BL/6 background, we utilized a multi-dose urethane model (1 g/kg weekly for 4 weeks) (84) to induce tumorigenesis in these mice. We observed a significant decrease in lung tumor incidence and multiplicity in Casp1 KO mice compared to WT mice (**Figure 23A-B**), indicating a role for caspase-1 (and likely inflammasome signaling) in lung carcinogenesis.
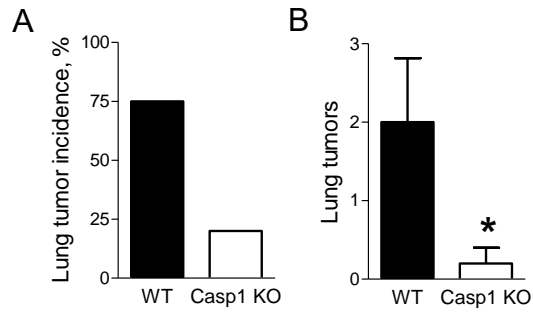
Figure 23: Deletion of caspase-1 reduces reduces lung tumor incidence and number. Complete caspase-1 knockout mice (Casp1 KO) and WT control mice on the C57BL/6 background were injected once weekly with urethane (1g/kg) for a total of 4 weeks. Mice were then maintained until harvest at week 16 after the first injection of urethane. A) Lung tumor incidence and (B) lung tumor number in Casp1 KO mice at 16 weeks after the first urethane injection (n=4-5 mice per group; *p<0.05 by Student's t-test compared to WT).

The role of inflammasome components and products in lung tumorigenesis has not been comprehensively studied. Since caspase-1 processes and activates the inflammasome products IL-1β and IL-18, both of which can promote tumorigenesis (230, 231), tumor studies almost always investigate caspase-1 for its role in inflammasome signaling. Thus, caspase-1 may mediate lung tumorigenesis through IL-1-mediated inflammatory mechanisms in immune cells. On the other hand, caspase-1 may also regulate survival/apoptosis of tumor cells, as has been described for colon cancer cells stimulated with IFNγ (232). A future direction of this work is to determine how caspase-1 promotes lung carcinogenesis and to identify other critical components of the inflammasome complex that are necessary for increased tumor formation. Two potentially important inflammasome scaffolding proteins in lung cancer may be AIM2 and NLRP3, which were recently found to be overexpressed in both lung cancer cell lines and lung cancer tissues from stage 1 lung cancer patients. NLRP3 was the most highly expressed scaffold protein in high-grade adenocarcinomas (228). Mutations in NLRP3 are present in 16% of lung adenocarcinomas, and these NLRP3-mutant lung tumors are enriched for NF-κB activity, suggesting that NLRP3 mutations as gain-of-function mutations that could promote cancer cell survival and/or mediate cancer-related inflammation (233). Very little is known about the role of AIM2 in lung cancer, but it may play a role in mediating immunosuppression in plasmacytoid dendritic cells (234). Another inflammasome component is the ASC adaptor protein, which is hypermethylated during late stages of lung cancer (235), indicating a potential role for inflammasome signaling in lung tumor progression and metastasis. ASC is thought to mediate tumor suppression under normal conditions by binding to IKKs and preventing inflammatory NF-κB signaling. However, under cancerous conditions, ASC binds to other subunits of the inflammasome complex, releasing IKK and allowing NF-κB activation. Low levels of ASC in advanced stage cancers are thought to be sequestered

into active inflammasome complexes so that unrestrained inflammatory signaling may occur (236). Because the field of inflammasome signaling is so new, there is much to be gained from investigating its potential role in facilitating lung tumorigenesis in order to identify additional targets for lung cancer treatment.

Role of cathepsin G in lung carcinogenesis

Our study shows that cathepsin G plays a role in lung tumorigenesis by processing pro-IL-1β in the context of NF-κB inhibition. This suggests that targeting cathepsin G might be of interest to overcome resistance to NF-κB inhibitor therapy. Very little is known about cathepsin G in lung cancer, and future studies will be necessary to determine its role in lung tumorigenesis with and without NF-κB inhibition. In lung cancer patients, cathepsin G expression in tumor-infiltrating neutrophils has been correlated with increasing disease grade and stage (206). A mouse model of lung metastasis showed that genetic co-deletion of cathepsin G and neutrophil elastase reduced lung metastases from LLC lung adenocarcinoma and B16-BL6 melanoma cells by degrading the anti-tumorigenic factor thrombospondin-1 (Tsp-1), suggesting that cathepsin G may play a role in lung metastasis (237). These two studies represent the only information currently available about cathepsin G in lung cancer. However, based on the literature, cathepsin G may also promote tumorigenesis through release/processing of chemotactic factors for inflammatory cell recruitment (238–240), angiogenesis via induction of TGFβ-mediated VEGF and CCL2 or via induction of endothelial-derived growth factors (241, 242), tumor cell invasion via activation of MMP2 (243), and formation of tumor cell aggregates, which are multicellular collections of tumor cells that can disseminate from the primary tumor and extravasate into the bloodstream or lymphatic system (244, 245). Another avenue of study that should be investigated is the relationship between NF-κB and cathepsin G. There is no current evidence that NF-κB regulates cathepsin G

75

expression. However, cathepsin G has been shown to cleave NF-κB subunit p65 in promyelocytic cells *in vitro*. It remains to be determined if this activity is relevant *in vivo*.

Conclusion

The work presented in this dissertation has broad implications for inflammatory signaling, lung cancer biology, and future therapeutics. Our studies have demonstrated that the role of NF-κB signaling in disease is variable depending on cell type and preexisting environmental conditions. In lung cancer, NF-κB is activated in most tumors and supports epithelial cell survival and growth (83, 84, 86–88), yet inhibitors of the NF-κB signaling pathway have little to no tumor effect in patients (101, 102). Our data suggest that the lack of response to NF-κB inhibitors is due to previously unrecognized pro-tumorigenic signaling in myeloid cells when NF-κB is suppressed. In other words, pro-tumor responses from NF-κB inhibition in myeloid cells counterbalance anti-tumor responses from NF-κB inhibition in epithelial cells such that the net effect of inhibitor therapy is negligible. Interestingly, the utility of a therapy appears to be related to its effect on inflammation, as reduction in inflammation leads to reduced tumors and vice versa in several different cancer models (78, 83, 84, 110, 176). In order to tip the balance toward an anti-tumor response to NF-κB inhibitor therapy, we identified and targeted the pro-tumorigenic mechanism of NF-κB-deficient myeloid cells during lung tumorigenesis. We found that neutrophils, a myeloid subpopulation, supported lung tumorigenesis by dysregulating processing of IL-1β through a novel cathepsin G-regulated mechanism. Processed and activated IL-1β provided survival signals to epithelial cells. Using a novel combination therapy with bortezomib and IL-1ra, we were able to reduce lung tumor formation and growth. Since both bortezomib and IL-1ra are clinically available, these results provide strong support for investigation of this

combination therapy in lung cancer patients. The successful response to bortezomib and

IL-1ra therapy in preclinical models emphasizes both the potential of and the need to

explore additional combinations of targeted therapies in cancer treatment. Our approach

to counteract mediators of resistance can be extended to other targeted therapies, such

as angiogenesis and checkpoint inhibitors and may prolong patient response and

improve survival.

REFERENCES

1. Siegel RL, Miller KD, Jemal A. Cancer statistics, 2015. *CA Cancer J Clin.* 2015;65(1):5–29.

2. U.S. Department of Health and Human Services. The health consequences of smoking — 50 years of progress: A report of the surgeon general. Rockville, MD: 2014: 1-1081.

3. American Cancer Society. Cancer facts & figures 2015. Atlanta, GA: 2015:1-52.

4. Mayo Clinic Staff. Lung cancer: Risk factors. Mayo Clinic Web Site. http://www.mayoclinic.org/diseases-conditions/lung-cancer/basics/risk-factors/con-20025531. Updated Septembe 25, 2015. Accessed January 4, 2016.

5. Travis W, Brambilla E, Müller-Hermelink H, Harris C. Pathology and fenetics: Tumours of the lung, pleura, thymus and heart. In: World Health Organization Classification of Tumours. Lyon, France: IARC Press; 2004:1–124.

6. American Cancer Society. What is non-small cell lung cancer? American Cancer Society Web Site. http://www.cancer.org/cancer/lungcancer-non-smallcell/detailedguide/non-small-cell-lung-cancer-what-is-non-small-cell-lung-cancer. Updated May 16, 2016. Accessed January 4, 2016.

7. Lemjabbar-Alaoui H, Hassan OU, Yang Y-W, Buchanan P. Lung cancer: Biology and treatment options. *Biochim Biophys Acta.* 2015;1856(2):189–210.

8. Hellenic Center for Disease Control and Prevention. Carcinoma of the lung: histopathology. *HCDCP Web Site.* http://www2.keelpno.gr/blog/?p=1391&lang=en. Updated February 22, 2012. Accessed January 4, 2016.

9. Travis WD, Brambilla E, Riely GJ. New pathologic classification of lung cancer: Relevance for clinical practice and clinical trials. *J Clin Oncol.* 2013;31(8):992–1001.

10. Stratton MR, Campbell PJ, Futreal PA. The cancer genome. *Nature.* 2009;458(7239):719–724.

11. Boolell V, Alamgeer M, Watkins DN, Ganju V. The evolution of therapies in non-small cell lung cancer. *Cancers (Basel).* 2015;7(3):1815–1846.

12. Pao W, Hutchinson KE. Chipping away at the lung cancer genome. *Nat Med.* 2012;18(3):349–351.

13. Tanoue LT, Detterbeck FC. New TNM classification for non-small-cell lung cancer. *Expert Rev Anticancer Ther.* 2009;9(4):413–423.

14. Sangha R, Price J, Butts CA. Adjuvant therapy in non-small cell lung cancer: Current and future directions. *Oncologist.* 2010;15(8):862–872.

15. National Comprehensive Cancer Network. National Comprehensive Cancer Network guidelines version 3.2016 non-small cell lung cancer. 2016:1-168.

16. Minguet J, Smith KH, Bramlage P. Targeted therapies for treatment of non-small cell lung cancer — recent advances and future perspectives. *Int J Cancer.* 2015;138(11):2549–2561.

17. Mitsudomi T et al. Gefitinib versus cisplatin plus docetaxel in patients with non-small-cell lung cancer harbouring mutations of the epidermal growth factor receptor (WJTOG3405): an open label, randomised phase 3 trial. *Lancet Oncol.* 2010;11(2):121–128.

18. Zhou C et al. Erlotinib versus chemotherapy as first-line treatment for patients with advanced EGFR mutation-positive non-small-cell lung cancer (OPTIMAL, CTONG-0802): a multicentre, open-label, randomised, phase 3 study. *Lancet Oncol.* 2011;12(8):735–742.

19. Rosell R et al. Erlotinib versus standard chemotherapy as first-line treatment for European patients with advanced EGFR mutation-positive non-small-cell lung cancer (EURTAC): a multicentre, open-label, randomised phase 3 trial. *Lancet Oncol.* 2012;13(3):239–246.

20. Inoue A et al. Updated overall survival results from a randomized phase III trial comparing gefitinib with carboplatin-paclitaxel for chemo-naïve non-small cell lung cancer with sensitive EGFR gene mutations (NEJ002). *Ann Oncol.* 2013;24(1):54–59.

21. Maemondo M et al. Gefitinib or chemotherapy for non-small-cell lung cancer with mutated EGFR. *N Engl J Med.* 2010;362(25):2380–2388.

22. Yu HA et al. Analysis of tumor specimens at the time of acquired resistance to EGFR-TKI therapy in 155 patients with EGFR-mutant lung cancers. *Clin Cancer Res.* 2013;19(8):2240–2247.

23. Inukai M et al. Presence of epidermal growth factor receptor gene T790M mutation as a minor clone in non-small cell lung cancer. *Cancer Res.* 2006;66(16):7854–7858.

24. Pao W et al. Acquired resistance of lung adenocarcinomas to gefitinib or erlotinib is associated with a second mutation in the EGFR kinase domain. *PLoS Med.* 2005;2(3):e73.

25. Yang JC-H et al. Afatinib for patients with lung adenocarcinoma and epidermal growth factor receptor mutations (LUX-Lung 2): a phase 2 trial. *Lancet Oncol.* 2012;13(5):539–548.

26. Sequist L V. et al. Phase III study of afatinib or cisplatin plus pemetrexed in patients with metastatic lung adenocarcinoma with EGFR mutations. *J Clin Oncol.* 2013;31(27):3327–3334.

27. Yang J, Ahn M, Ramalingam S, Al. E. AZD9291 in pre-treated T790M positive advanced NSCLC: AURA study phase II extension cohort. In: 16th World Conference on Lung Cancer. Denver, CO: Abstract 943.

28. Mitsudomi T, Tsai C, Shepherd F, Al. E. AZD9291 in pre-treated T790M positive advanced NSCLC: AURA2 phase II study. In: 16th World Conference on Lung Cancer. Denver, CO: Abstract 1406.

29. Jänne PA et al. AZD9291 in EGFR inhibitor-resistant non-small-cell lung cancer. *N Engl J Med.* 2015;372(18):1689–1699.

30. Shaw AT et al. Crizotinib versus chemotherapy in advanced ALK-positive lung cancer. *N Engl J Med.* 2013;368(25):2385–2394.

31. Solomon BJ et al. First-line crizotinib versus chemotherapy in ALK-positive lung cancer. *N Engl J Med.* 2014;371(23):2167–2177.

32. Kwak EL et al. Anaplastic lymphoma kinase inhibition in non-small-cell lung cancer. *N Engl J Med.* 2010;363(18):1693–1703.

33. Camidge DR et al. Activity and safety of crizotinib in patients with ALK-positive non-small-cell lung cancer: Updated results from a phase 1 study. *Lancet Oncol.* 2012;13(10):1011–1019.

34. Shaw AT et al. Ceritinib in ALK-rearranged non-small-cell lung cancer. *N Engl J Med.* 2014;370(13):1189–1197.

35. Ou S-HI et al. Alectinib in crizotinib-refractory ALK-rearranged non-small-cell lung cancer: A phase II global study. *J Clin Oncol.* 2015;34(7):661–668.

36. Nishida N, Yano H, Nishida T, Kamura T, Kojiro M. Angiogenesis in cancer. *Vasc Health Risk Manag.* 2006;2(3):213–219.

37. Johnson DH. Randomized phase II trial comparing bevacizumab plus carboplatin and paclitaxel with carboplatin and paclitaxel alone in previously untreated locally advanced or metastatic non-small-cell lung cancer. *J Clin Oncol.* 2004;22(11):2184–2191.

38. Reck M et al. Overall survival with cisplatin-gemcitabine and bevacizumab or placebo as first-line therapy for nonsquamous non-small-cell lung cancer: Results from a randomised phase III trial (AVAiL). *Ann Oncol.* 2010;21(9):1804–1809.

39. Sandler A et al. Paclitaxel-carboplatin alone or with bevacizumab for non-small-cell lung cancer. *N Engl J Med.* 2006;355(24):2542–2550.

40. Reck M et al. Docetaxel plus nintedanib versus docetaxel plus placebo in patients with previously treated non-small-cell lung cancer (LUME-Lung 1): A phase 3, double-blind, randomised controlled trial. *Lancet Oncol.* 2014;15(2):143–155.

41. Huang Y, Carbone DP. Mechanisms of and strategies for overcoming resistance to anti-vascular endothelial growth factor therapy in non-small cell lung cancer. *Biochim Biophys Acta.* 2015;1855(2):193–201.

42. Pardoll DM. The blockade of immune checkpoints in cancer immunotherapy. *Nat Rev Cancer.* 2012;12(4):252–264.

43. Brahmer JR et al. Phase I study of single-agent anti-programmed death-1 (MDX-1106) in refractory solid tumors: Safety, clinical activity, pharmacodynamics, and immunologic correlates. *J Clin Oncol.* 2010;28(19):3167–3175.

44. Brahmer JR et al. Safety and activity of anti-PD-L1 antibody in patients with advanced cancer. *N Engl J Med.* 2012;366(26):2455–2465.

45. Topalian SL et al. Safety, activity, and immune correlates of anti-PD-1 antibody in cancer. *N Engl J Med.* 2012;366(26):2443–2454.

46. Borghaei H et al. Nivolumab versus docetaxel in advanced nonsquamous non-small-cell lung cancer. *N Engl J Med.* 2015;373(17):1627–1639.

47. Brahmer J et al. Nivolumab versus docetaxel in advanced squamous-cell non-small-cell lung cancer. *N Engl J Med.* 2015;373(2):123–135.

48. Garon EB et al. Pembrolizumab for the treatment of non-small-cell lung cancer. *N Engl J Med.* 2015;372(21):2018–2028.

49. Bristol Myers Squibb. Bristol-Myers Squibb announces top-line results from checkmate -026, a phase 3 study of Opdivo (nivolumab) in treatment-naïve patients with advanced non-small cell lung cancer. Bristol Myers Squibb Web Site. http://news.bms.com/press-release/bristolmyers/bristol-myers-squibb-announces-top-line-results-checkmate-026-phase-3-stu. Updated August 5, 2016. Accessed September 19, 2016.

50. Fennell D. Expert Opinion — The challenges of lung cancer. Cancer Research UK Web Site. http://scienceblog.cancerresearchuk.org/2013/04/04/expert-opinion-the-challenges-of-lung-cancer/. Updated April 4, 2013. Accessed January 6, 2016.

51. Aberle DR et al. Reduced lung-cancer mortality with low-dose computed tomographic screening. *N Engl J Med.* 2011;365(5):395–409.

52. Rothschild SI. Targeted therapies in non-small cell lung cancer — beyond EGFR and ALK. *Cancers (Basel).* 2015;7(2):930–949.

53. Creelan BC. Update on immune checkpoint inhibitors in lung cancer. *Cancer Control* 2014;21(1):80–89.

54. Colotta F, Allavena P, Sica A, Garlanda C, Mantovani A. Cancer-related inflammation, the seventh hallmark of cancer: Links to genetic instability. *Carcinogenesis.* 2009;30(7):1073–1081.

55. Baud V, Karin M. Is NF-kappaB a good target for cancer therapy? Hopes and pitfalls. *Nat Rev Drug Discov.* 2009;8(1):33–40.

56. Martinka S, Bruggeman LA. Persistent NF-kappaB activation in renal epithelial cells in a mouse model of HIV-associated nephropathy. *Am J Physiol Renal Physiol.* 2006;290(3):F657–F665.

57. Sethi G, Shanmugam MK, Ramachandran L, Kumar AP, Tergaonkar V. Multifaceted link between cancer and inflammation. *Biosci Rep.* 2012;32(1):1–15.

58. Oeckinghaus A, Ghosh S. The NF-kappaB family of transcription factors and its regulation. *Cold Spring Harb Perspect Biol.* 2009;1(4):a000034.

59. Sun S-C. The noncanonical NF-κB pathway. *Immunol Rev.* 2012;246(1):125–140.

60. Annunziata CM et al. Frequent engagement of the classical and alternative NF-kappaB pathways by diverse genetic abnormalities in multiple myeloma. *Cancer Cell.* 2007;12(2):115–130.

61. Keats JJ et al. Promiscuous mutations activate the noncanonical NF-kappaB pathway in multiple myeloma. *Cancer Cell.* 2007;12(2):131–144.

62. Chapman MA et al. Initial genome sequencing and analysis of multiple myeloma. *Nature.* 2011;471(7339):467–472.

63. Willis TG et al. Bcl10 is involved in t(1;14)(p22;q32) of MALT B cell lymphoma and mutated in multiple tumor types. *Cell.*1999;96(1):35–45.

64. Uren AG et al. Identification of paracaspases and metacaspases: Two ancient families of caspase-like proteins, one of which plays a key role in MALT lymphoma. *Mol Cell.* 2000;6(4):961–967.

65. Lenz G et al. Oncogenic CARD11 mutations in human diffuse large B cell lymphoma. *Science.* 2008;319(5870):1676–1679.

66. Ngo VN et al. Oncogenically active MYD88 mutations in human lymphoma. *Nature.* 2010;470(7332):115–119.

67. Tichelaar JW et al. Increased staining for phospho-Akt, p65/RELA and cIAP-2 in pre-neoplastic human bronchial biopsies. *BMC Cancer.* 2005;5:155.

68. Erstad DJ, Cusack JC. Targeting the NF-κB pathway in cancer therapy. *Surg Oncol Clin N Am.* 2013;22(4):705–746.

69. Jin X et al. Potential biomarkers involving IKK/RelA signal in early stage non-small cell lung cancer. *Cancer Sci.* 2008;99(3):582–589.

70. Brose MS et al. BRAF and RAS mutations in human lung cancer and melanoma. *Cancer Res.* 2002;62(23):6997–7000.

71. Davies H et al. Somatic mutations of the protein kinase gene family in human lung cancer. *Cancer Res.* 2005;65(17):7591–7595.

72. Paez JG et al. EGFR mutations in lung cancer: Correlation with clinical response to gefitinib therapy. *Science.* 2004;304(5676):1497–1500.

73. Sher T, Dy GK, Adjei AA. Small cell lung cancer. *Mayo Clin Proc.* 2008;83(3):355–367.

74. Stephens P et al. Lung cancer: Intragenic ERBB2 kinase mutations in tumours. *Nature.* 2004;431(7008):525–526.

75. Tsurutani J. Tobacco components stimulate Akt-dependent proliferation and NFκB-dependent survival in lung cancer cells. *Carcinogenesis.* 2004;26(7):1182–1195.

76. Smith CJ, Perfetti TA, King JA. Perspectives on pulmonary inflammation and lung cancer risk in cigarette smokers. *Inhal Toxicol.* 2006;18(9):667–677.

77. Karin M. NF-κB as a Critical link between inflammation and cancer. *Cold Spring Harb Perspect Biol.* 2009;1(5):a000141–a000141.

78. Greten FR et al. IKKbeta links inflammation and tumorigenesis in a mouse model of colitis-associated cancer. *Cell.* 2004;118(3):285–296.

79. Sakamoto K et al. Inhibitor of kappaB kinase beta regulates gastric carcinogenesis via interleukin-1alpha expression. *Gastroenterology.* 2010;139(1):226–238.

80. Pikarsky E et al. NF-kappaB functions as a tumour promoter in inflammation-associated cancer. *Nature.* 2004;431(7007):461–466.

81. Yang J et al. Conditional ablation of Ikkb inhibits melanoma tumor development in mice. *J Clin Invest.* 2010;120(7):2563–2574.

82. Zaynagetdinov R et al. Chronic NF-κB activation links COPD and lung cancer through generation of an immunosuppressive microenvironment in the lungs. *Oncotarget.* 2016;7(5):5470–5482.

83. Zaynagetdinov R et al. Epithelial nuclear factor-κB signaling promotes lung carcinogenesis via recruitment of regulatory T lymphocytes. *Oncogene.* 2012;31(26):3164–3176.

84. Stathopoulos GT et al. Epithelial NF-kappaB activation promotes urethane-induced lung carcinogenesis. *Proc Natl Acad Sci USA.* 2007;104(47):18514–18519.

85. Saxon JA et al. Epithelial NF-κB signaling promotes EGFR-driven lung carcinogenesis via macrophage recruitment. *Oncoimmunology.* 2016;5(6):e1168549.

86. Bassères DS, Ebbs A, Levantini E, Baldwin AS. Requirement of the NF-{kappa}B subunit p65/RelA for K-ras-induced lung tumorigenesis. *Cancer Res.* 2010;(18):3537–3546.

87. Meylan E et al. Requirement for NF-kappaB signalling in a mouse model of lung adenocarcinoma. *Nature.* 2009;462(7269):104–107.

88. Xia Y et al. Reduced cell proliferation by IKK2 depletion in a mouse lung-cancer model. *Nat Cell Biol.* 2012;14(3):257–265.

89. Gilmore TD, Herscovitch M. Inhibitors of NF-κB signaling: 785 and counting. *Oncogene.* 2006;25(51):6887–6899.

90. U.S. Food & Drug Administration. Velcade (bortezomib) is approved for initial treatment of patients with multiple myeloma *U.S. Food & Drug Administration Web Site.* http://www.fda.gov/AboutFDA/CentersOffices/OfficeofMedicalProductsandTobacco/CDER/ucm094633.htm. Updated December 29, 2015. Accessed January 9, 2016.

91. Jones DR, Broad RM, Madrid L V, Baldwin AS, Mayo MW. Inhibition of NF-kappaB sensitizes non-small cell lung cancer cells to chemotherapy-induced apoptosis. *Ann Thorac Surg.* 2000;70(3):930–937.

92. Cheng Q, Lee HH, Li Y, Parks TP, Cheng G. Upregulation of Bcl-x and Bfl-1 as a potential mechanism of chemoresistance, which can be overcome by NF-κB inhibition. *Oncogene.* 2000;19(42):4936–4940.

93. Denlinger CE, Rundall BK, Keller MD, Jones DR. Proteasome inhibition sensitizes non–small-cell lung cancer to gemcitabine-induced apoptosis. *Ann Thorac Surg.* 2004;78(4):1207–1214.

94. Davies AM, Lara PN, Mack PC, Gandara DR. Incorporating bortezomib into the treatment of lung cancer. *Clin Cancer Res.* 2007;13(15):4647s–4651s.

95. Escobar M, Velez M, Belalcazar A, Santos ES, Raez LE. The role of proteasome inhibition in nonsmall cell lung cancer. *J Biomed Biotechnol.* 2011;2011:1–10.

96. Hoang T et al. Vorinostat and bortezomib as third-line therapy in patients with advanced non-small cell lung cancer: A Wisconsin Oncology Network phase II study. *Invest New Drugs.* 2014;32(1):195–199.

97. Lara PN et al. Randomized phase II Trial of concurrent versus sequential bortezomib plus docetaxel in advanced non–small-cell lung cancer: A California Cancer Consortium trial. *Clin Lung Cancer.* 2011;12(1):33–37.

98. Piperdi B et al. Phase-I/II study of bortezomib in combination with carboplatin and bevacizumab as first-line therapy in patients with advanced non-small-cell lung cancer. *J Thorac Oncol.* 2012;7(6):1032–1040.

99. Ramalingam SS et al. Bortezomib for patients with advanced-stage bronchioloalveolar carcinoma: A California Cancer Consortium phase II study (NCI 7003). *J Thorac Oncol.* 2011;6(10):1741–1745.

100. Zhao Y et al. A phase I/II study of bortezomib in combination with paclitaxel, carboplatin, and concurrent thoracic radiation therapy for non–small-cell lung cancer. *J Thorac Oncol.* 2015;10(1):172–180.

101. Besse B et al. Phase 2 study of frontline bortezomib in patients with advanced non-small cell lung cancer. *Lung Cancer.* 2012;76(1):78–83.

102. Fanucchi MP et al. Randomized phase II study of bortezomib alone and bortezomib in combination with docetaxel in previously treated advanced non-small-cell lung cancer. *J Clin Oncol.* 2006;24(31):5025–5033.

103. Wang X, Chen W, Lin Y. Sensitization of TNF-induced cytotoxicity in lung cancer cells by concurrent suppression of the NF-κB and Akt pathways. *Biochem Biophys Res Commun.* 2007;355(3):807–812.

104. Wang X. 17-Allylamino-17-Demethoxygeldanamycin synergistically potentiates tumor necrosis factor-induced lung cancer cell death by blocking the nuclear factor-κB pathway. *Cancer Res.* 2006;66(2):1089–1095.

105. Chen W et al. Blockage of NF-κB by IKKβ- or RelA-siRNA rather than the NF-κB super-suppressor IκBα mutant potentiates adriamycin-induced cytotoxicity in lung cancer cells. *J Cell Biochem.* 2008;105(2):554–561.

106. Ju W et al. A critical role of luteolin-induced reactive oxygen species in blockage of tumor necrosis factor-activated nuclear factor-kappaB pathway and sensitization of apoptosis in lung cancer cells. *Mol Pharmacol.* 2007;71(5):1381–1388.

107. Li Y. Inactivation of nuclear factor κB by soy isoflavone genistein contributes to increased apoptosis induced by chemotherapeutic agents in human cancer cells. *Cancer Res.* 2005;65(15):6934–6942.

108. Bassères DS, Ebbs A, Cogswell PC, Baldwin AS. IKK is a therapeutic target in KRAS-Induced lung cancer with disrupted p53 activity. *Genes Cancer.* 2014;5(1-2):41–55.

109. Xue W et al. Response and resistance to NF-κB inhibitors in mouse models of lung adenocarcinoma. *Cancer Discov.* 2011;1(3):236–247.

110. Karabela SP et al. Opposing effects of bortezomib-induced nuclear factor-κB inhibition on chemical lung carcinogenesis. *Carcinogenesis.* 2012;33(4):859–867.

111. Martin TR, Frevert CW. Innate immunity in the lungs. *Proc Am Thorac Soc.* 2005;2(5):403–411.

112. Kindt T, Goldsby R, Osborne B. Innate immunity. In: Ahr K ed. Immunology. New York, NY: W.H. Freeman and Company; 2007:65–69.

113. Rajnavolgyi E et al. Tumor associated macrophages and neutrophils in cancer. *Immunobiology.* 2013;218(11):1402–1410.

114. Caronni N, Savino B, Bonecchi R. Myeloid cells in cancer-related inflammation.. *Immunobiology.* 2015;220(2):249–253.

115. Mantovani A, Sozzani S, Locati M, Allavena P, Sica A. Macrophage polarization: tumor-associated macrophages as a paradigm for polarized M2 mononuclear phagocytes. *Trends Immunol.* 2002;23(11):549–555.

116. Talmadge JE, Donkor M, Scholar E. Inflammatory cell infiltration of tumors: Jekyll or Hyde. *Cancer Metastasis Rev.* 2007;26(3-4):373–400.

117. Pollard JW. Tumour-educated macrophages promote tumour progression and metastasis. *Nat Rev Cancer.* 2004;4(1):71–78.

118. Biswas SK et al. A distinct and unique transcriptional program expressed by tumor-associated macrophages (defective NF-kappaB and enhanced IRF-3/STAT1 activation). *Blood.* 2006;107(5):2112–2122.

119. Sica A, Schioppa T, Mantovani A, Allavena P. Tumour-associated macrophages are a distinct M2 polarised population promoting tumour progression: Potential targets of anti-cancer therapy. *Eur J Cancer.* 2006;42(6):717–727.

120. Welsh TJ et al. Macrophage and mast-cell invasion of tumor cell islets confers a marked survival advantage in non-small-cell lung cancer. *J Clin Oncol.* 2005;23(35):8959–8967.

121. Kim D-W et al. High tumour islet macrophage infiltration correlates with improved patient survival but not with EGFR mutations, gene copy number or protein expression in resected non-small cell lung cancer. *Br J Cancer.* 2008;98(6):1118–1124.

122. Dai F et al. The number and microlocalization of tumor-associated immune cells are associated with patient's survival time in non-small cell lung cancer. *BMC Cancer.* 2010;10:220.

123. Ma J et al. The M1 form of tumor-associated macrophages in non-small cell lung cancer is positively associated with survival time. *BMC Cancer.* 2010;10:112.

124. Ohri CM, Shikotra A, Green RH, Waller DA, Bradding P. Macrophages within NSCLC tumour islets are predominantly of a cytotoxic M1 phenotype associated with extended survival. *Eur Respir J.* 2009;33(1):118–126.

125. Chung F-T et al. Tumor-associated macrophages correlate with response to epidermal growth factor receptor-tyrosine kinase inhibitors in advanced non-small cell lung cancer. *Int J Cancer.* 2012;131(3):E227–E235.

126. Ohtaki Y et al. Stromal macrophage expressing CD204 is associated with tumor aggressiveness in lung adenocarcinoma. *J Thorac Oncol.* 2010;5(10):1507–1515.

127. Zhang B et al. M2-polarized tumor-associated macrophages are associated with poor prognoses resulting from accelerated lymphangiogenesis in lung adenocarcinoma. *Clinics (São Paulo, Brazil).* 2011;66(11):1879–1886.

128. Jablonska J, Leschner S, Westphal K, Lienenklaus S, Weiss S. Neutrophils responsive to endogenous IFN-beta regulate tumor angiogenesis and growth in a mouse tumor model. *J Clin Invest.* 2010;120(4):1151–1164.

129. Andzinski L et al. Type I IFNs induce anti-tumor polarization of tumor associated neutrophils in mice and human. *Int J Cancer.* 2015;138(8):1982–1993.

130. Fridlender ZG et al. Polarization of tumor-associated neutrophil phenotype by TGF-beta: "N1" versus "N2" TAN. *Cancer Cell.* 2009;16(3):183–194.

131. Lichtenstein A, Seelig M, Berek J, Zighelboim J. Human neutrophil-mediated lysis of ovarian cancer cells. *Blood.* 1989;74(2):805–809.

132. Zivkovic M et al. Oxidative burst of neutrophils against melanoma B16-F10. *Cancer Lett.* 2007;246(1-2):100–108.

133. Chen Y-L, Chen S-H, Wang J-Y, Yang B-C. Fas ligand on tumor cells mediates inactivation of neutrophils. *J Immunol.* 2003;171(3):1183–1191.

134. Beauvillain C et al. Neutrophils efficiently cross-prime naive T cells in vivo. *Blood.* 2007;110(8):2965–2973.

135. Kousis PC, Henderson BW, Maier PG, Gollnick SO. Photodynamic therapy enhancement of antitumor immunity is regulated by neutrophils. *Cancer Res.* 2007;67(21):10501–10510.

136. Scapini P et al. The neutrophil as a cellular source of chemokines. *Immunol Rev.* 2000;177(1):195–203.

137. Cavallo F et al. Role of neutrophils and CD4+ T lymphocytes in the primary and memory response to nonimmunogenic murine mammary adenocarcinoma made immunogenic by IL-2 gene. *J Immunol.* 1992;149(11):3627–3635.

138. Fridlender ZG, Albelda SM. Tumor-associated neutrophils: friend or foe?. *Carcinogenesis.* 2012;33(5):949–955.

139. Rodriguez PC et al. Arginase I production in the tumor microenvironment by mature myeloid cells inhibits T-cell receptor expression and antigen-specific T-cell responses. *Cancer Res.* 2004;64(16):5839–5849.

140. Rotondo R et al. IL-8 induces exocytosis of arginase 1 by neutrophil polymorphonuclears in nonsmall cell lung cancer. *Int J Cancer.* 2009;125(4):887–893.

141. Izhak L et al. Dissecting the autocrine and paracrine roles of the CCR2-CCL2 axis in tumor survival and angiogenesis. *PLoS One.* 2012;7(1):e28305.

142. Ma J, Wang Q, Fei T, Han J-DJ, Chen Y-G. MCP-1 mediates TGF-beta-induced angiogenesis by stimulating vascular smooth muscle cell migration. *Blood.* 2007;109(3):987–994.

143. Aldinucci D, Colombatti A. The inflammatory chemokine CCL5 and cancer progression. *Mediators Inflamm.* 2014;2014:292376.

144. Thanee M, Yongvanit P, Loilome W. Search Tumor Microenvironment and its Functions. *Srinagarind Med J.* 2012;27(4).

145. Teramukai S et al. Pretreatment neutrophil count as an independent prognostic factor in advanced non-small-cell lung cancer: An analysis of Japan Multinational Trial Organisation LC00-03. *Eur J Cancer.* 2009;45(11):1950–1958.

146. Paesmans M et al. Prognostic factors for survival in advanced non-small-cell lung cancer: univariate and multivariate analyses including recursive partitioning and amalgamation algorithms in 1,052 patients. The European Lung Cancer Working Party. *J Clin Oncol.* 1995;13(5):1221–1230.

147. Tibaldi C et al. Baseline elevated leukocyte count in peripheral blood is associated with poor survival in patients with advanced non-small cell lung cancer: A prognostic model. *J Cancer Res Clin Oncol.* 2008;134(10):1143–1149.

148. Di Maio M et al. Chemotherapy-induced neutropenia and treatment efficacy in advanced non-small-cell lung cancer: A pooled analysis of three randomised trials. *Lancet Oncol.* 2005;6(9):669–677.

149. Sionov RV, Fridlender ZG, Granot Z. The multifaceted roles neutrophils play in the tumor microenvironment. *Cancer Microenviron.* 2015;8(3):125–158.

150. Ilie M et al. Predictive clinical outcome of the intratumoral CD66b-positive neutrophil-to-CD8-positive T-cell ratio in patients with resectable nonsmall cell lung cancer. *Cancer.* 2012;118(6):1726–1737.

151. Eruslanov EB et al. Tumor-associated neutrophils stimulate T cell responses in early-stage human lung cancer. *J Clin Invest.* 2014;124(12):5466–5480.

152. Mucha J, Majchrzak K, Taciak B, Hellmén E, Król M. MDSCs mediate angiogenesis and predispose canine mammary tumor cells for metastasis via IL-28/IL-28RA (IFN-λ) signaling. *PLoS One.* 2014;9(7):e103249.

153. Meirow Y, Kanterman J, Baniyash M. Paving the road to tumor development and spreading: Myeloid-derived suppressor cells are ruling the fate. *Front Immunol.* 2015;6:523.

154. Zhang G et al. A novel subset of B7-H3(+)CD14(+)HLA-DR(-/low) myeloid-derived suppressor cells are associated with progression of human NSCLC. *Oncoimmunology.* 2015;4(2):e977164.

155. Li Z-L et al. COX-2 promotes metastasis in nasopharyngeal carcinoma by mediating interactions between cancer cells and myeloid-derived suppressor cells. *Oncoimmunology.* 2015;4(11):e1044712.

156. Huang H, Zhang G, Li G, Ma H, Zhang X. Circulating CD14(+)HLA-DR(-/low) myeloid-derived suppressor cell is an indicator of poor prognosis in patients with ESCC. *Tumour Biol.* 2015;36(10):7987–7996.

157. Kusmartsev SA, Li Y, Chen SH. Gr-1+ myeloid cells derived from tumor-bearing mice inhibit primary T cell activation induced through CD3/CD28 costimulation. *J Immunol.* 2000;165(2):779–785.

158. Gabrilovich D et al. Vascular endothelial growth factor inhibits the development of dendritic cells and dramatically affects the differentiation of multiple hematopoietic lineages in vivo. *Blood.* 1998;92(11):4150–4166.

159. Watson GA, Fu YX, Lopez DM. Splenic macrophages from tumor-bearing mice co-expressing MAC-1 and MAC-2 antigens exert immunoregulatory functions via two distinct mechanisms. *J Leukoc Biol.* 1991;49(2):126–138.

160. Gabrilovich DI, Ostrand-Rosenberg S, Bronte V. Coordinated regulation of myeloid cells by tumours. *Nat Rev Immunol.* 2012;12(4):253–268.

161. Liu C-Y et al. Population alterations of L-arginase- and inducible nitric oxide synthase-expressed CD11b+/CD14⁻/CD15+/CD33+ myeloid-derived suppressor cells and CD8+ T lymphocytes in patients with advanced-stage non-small cell lung cancer. *J Cancer Res Clin Oncol.* 2010;136(1):35–45.

162. Pyzer AR, Cole L, Rosenblatt J, Avigan DE. Myeloid-derived suppressor cells as effectors of immune suppression in cancer. *Int J Cancer.* 2016;139(9):1915–1926.

163. Noman MZ et al. PD-L1 is a novel direct target of HIF-1α, and its blockade under hypoxia enhanced MDSC-mediated T cell activation. *J Exp Med.* 2014;211(5):781–790.

164. Bogdan C. Nitric oxide and the immune response. *Nat Immunol.* 2001;2(10):907–916.

165. Wu G, Morris SM. Arginine metabolism: Nitric oxide and beyond. *Biochem J.* 1998;1–17.

166. Rodriguez PC, Quiceno DG, Ochoa AC. L-arginine availability regulates T-lymphocyte cell-cycle progression. *Blood.* 2007;109(4):1568–1573.

167. Oberlies J et al. Regulation of NK cell function by human granulocyte arginase. *J Immunol.* 2009;182(9):5259–5267.

168. Bingisser RM, Tilbrook PA, Holt PG, Kees UR. Macrophage-derived nitric oxide regulates T cell activation via reversible disruption of the Jak3/STAT5 signaling pathway. *J Immunol.* 1998;160(12):5729–5734.

169. Harari O, Liao JK. Inhibition of MHC II gene transcription by nitric oxide and antioxidants. *Curr Pharm Des.* 2004;10(8):893–898.

170. Schmielau J, Finn OJ. Activated granulocytes and granulocyte-derived hydrogen peroxide are the underlying mechanism of suppression of t-cell function in advanced cancer patients. *Cancer Res.* 2001;61(12):4756–4760.

171. Nagaraj S et al. Altered recognition of antigen is a mechanism of CD8+ T cell tolerance in cancer. *Nat Med.* 2007;13(7):828–835.

172. Mannick JB et al. Fas-induced caspase denitrosylation. *Science.* 1999;284(5414):651–654.

173. Hoechst B, Gamrekelashvili J, Manns MP, Greten TF, Korangy F. Plasticity of human Th17 cells and iTregs is orchestrated by different subsets of myeloid cells. *Blood.* 2011;117(24):6532–6541.

174. Hoechst B et al. A new population of myeloid-derived suppressor cells in hepatocellular carcinoma patients induces CD4(+)CD25(+)Foxp3(+) T cells. *Gastroenterology.* 2008;135(1):234–243.

175. Sinha P, Clements VK, Bunt SK, Albelda SM, Ostrand-Rosenberg S. Cross-talk between myeloid-derived suppressor cells and macrophages subverts tumor immunity toward a type 2 response. *J Immunol.* 2007;179(2):977–983.

176. Takahashi H, Ogata H, Nishigaki R, Broide DH, Karin M. Tobacco smoke promotes lung tumorigenesis by triggering IKKbeta- and JNK1-dependent inflammation. *Cancer Cell.* 2010;17(1):89–97.

177. Hagemann T et al. "Re-educating" tumor-associated macrophages by targeting NF-kappaB. *J Exp Med.* 2008;205(6):1261–1268.

178. Fong CHY et al. An antiinflammatory role for IKKbeta through the inhibition of "classical" macrophage activation. *J Exp Med.* 2008;205(6):1269–1276.

179. Yang J et al. Myeloid IKKβ Promotes anti-tumor immunity by modulating ccl11 and the innate immune response. *Cancer Res.* 2014;74(24):7274–7284.

180. Enzler T et al. Cell-selective inhibition of NF-κB signaling improves therapeutic index in a melanoma chemotherapy model. *Cancer Discov.* 2011;1(6):496–507.

181. Li Z-W, Omori SA, Labuda T, Karin M, Rickert RC. IKK beta is required for peripheral B cell survival and proliferation. *J Immunol.* 2003;170(9):4630–4637.

182. Tuveson DA et al. Endogenous oncogenic K-ras(G12D) stimulates proliferation and widespread neoplastic and developmental defects. *Cancer Cell.* 2004;5(4):375–387.

183. Fisher GH et al. Induction and apoptotic regression of lung adenocarcinomas by regulation of a K-Ras transgene in the presence and absence of tumor suppressor genes. *Genes Dev.* 2001;15(24):3249–3262.

184. Everhart MB et al. Duration and intensity of NF-κB activity determine the severity of endotoxin-induced acute lung injury. *J Immunol.* 2006;176(8):4995–5005.

185. Feldman J, Goldwasser R, Shlomo M, Schwartz J, Itzhak O. A mathematical model for tumor volume evaluation using two dimensions. *J Appl Quant Methods.* 2009;4(4):455–462.

186. Zaynagetdinov R et al. A critical role for macrophages in promotion of urethane-induced lung carcinogenesis. *J Immunol.* 2011;187(11):5703–5711.

187. Lin Y, Bai L, Chen W, Xu S. The NF-kappaB activation pathways, emerging molecular targets for cancer prevention and therapy. *Expert Opin Ther Targets.* 2010;14(1):45–55.

188. Chen W, Li Z, Bai L, Lin Y. NF-kappaB in lung cancer, a carcinogenesis mediator and a prevention and therapy target. *Front Biosci. (Landmark ed)* 2011;16:1172–1185.

189. Stathopoulos GT et al. Host-derived interleukin-5 promotes adenocarcinoma-induced malignant pleural effusion. *Am J Respir Crit Care Med.* 2010;182(10):1273–1281.

190. Giannou AD et al. Mast cells mediate malignant pleural effusion formation. *J Clin Invest.* 2015;125(6):2317–2334.

191. Greten FR et al. NF-kappaB is a negative regulator of IL-1beta secretion as revealed by genetic and pharmacological inhibition of IKKbeta. *Cell.* 2007;130(5):918–931.

192. You M, Candrian U, Maronpot RR, Stoner GD, Anderson MW. Activation of the Ki-ras protooncogene in spontaneously occurring and chemically induced lung tumors of the strain A mouse. *Proc Natl Acad Sci USA.* 1989;86(9):3070–3074.

193. Westcott PMK et al. The mutational landscapes of genetic and chemical models of Kras-driven lung cancer. *Nature.* 2014;517(7535):489–492.

194. Fleming TJ, Fleming ML, Malek TR. Selective expression of Ly-6G on myeloid lineage cells in mouse bone marrow. RB6-8C5 mAb to granulocyte-differentiation antigen (Gr-1) detects members of the Ly-6 family. *J Immunol.* 1993;151(5):2399–2408.

195. Gabrilovich DI, Nagaraj S. Myeloid-derived suppressor cells as regulators of the immune system. *Nat Rev Immunol.* 2009;9(3):162–174.

196. Chen L-C et al. Tumour inflammasome-derived IL-1β recruits neutrophils and improves local recurrence-free survival in EBV-induced nasopharyngeal carcinoma. *EMBO Mol Med.* 2012;4(12):1276–1293.

197. Hsu L-C et al. IL-1β-driven neutrophilia preserves antibacterial defense in the absence of the kinase IKKβ. *Nat Immunol.* 2011;12(2):144–150.

198. Langereis JD, Raaijmakers HAJA, Ulfman LH, Koenderman L. Abrogation of NF-κB signaling in human neutrophils induces neutrophil survival through sustained p38-MAPK activation. *J Leukoc Biol.* 2010;88(4):655–664.

199. Houghton AM et al. Neutrophil elastase-mediated degradation of IRS-1 accelerates lung tumor growth. *Nat Med.* 2010;16(2):219–223.

200. Gong L et al. Promoting effect of neutrophils on lung tumorigenesis is mediated by CXCR2 and neutrophil elastase. *Mol Cancer.* 2013;12(1):154.

201. Lind H, Haugen A, Zienolddiny S. Differential binding of proteins to the IL1B -31 T/C polymorphism in lung epithelial cells. *Cytokine.* 2007;38(1):43–48.

202. Li C, Wang C. Current evidences on IL1B polymorphisms and lung cancer susceptibility: a meta-analysis. *Tumour Biol.* 2013;34(6):3477–3482.

203. Cogswell JP et al. NF-kappa B regulates IL-1 beta transcription through a consensus NF-kappa B binding site and a nonconsensus CRE-like site. *J Immunol.* 1994;153(2):712–723.

204. Huang HJ et al. Maintenance of IKKβ activity is necessary to protect lung grafts from acute injury. *Transplantation.* 2011;91(6):624–631.

205. Guma M et al. Caspase 1-independent activation of interleukin-1beta in neutrophil-predominant inflammation. *Arthritis Rheum.* 2009;60(12):3642–3650.

206. Maksimowicz T et al. Activity and tissue localization of cathepsin G in non small cell lung cancer. *Rocz Akad Med w Białymstoku.* 1997;42 Suppl 1:199–216.

207. Gibbs JB. Mechanism-based target identification and drug discovery in cancer research. *Science.* 2000;287(5460):1969–73.

208. DeBusk LM, Massion PP, Lin PC. IkappaB kinase-alpha regulates endothelial cell motility and tumor angiogenesis. *Cancer Res.* 2008;68(24):10223–10228.

209. Huang S, Robinson JB, Deguzman A, Bucana CD, Fidler IJ. Blockade of nuclear factor-kappaB signaling inhibits angiogenesis and tumorigenicity of human ovarian cancer cells by suppressing expression of vascular endothelial growth factor and interleukin 8. *Cancer Res.* 2000;60(19):5334–5339.

210. Schmidt D et al. Critical role for NF-kappaB-induced JunB in VEGF regulation and tumor angiogenesis. *EMBO J.* 2007;26(3):710–719.

211. Lee D-F et al. IKK beta suppression of TSC1 links inflammation and tumor angiogenesis via the mTOR pathway. *Cell.* 2007;130(3):440–455.

212. Sunderkotter C, Steinbrink K, Goebeler M, Bhardwaj R, Sorg C. Macrophages and angiogenesis. *J Leukoc Biol.* 1994;55(3):410–422.

213. Fujioka S et al. NF-kappaB and AP-1 connection: Mechanism of NF-kappaB-dependent regulation of AP-1 activity. *Mol Cell Biol.* 2004;24(17):7806–7819.

214. Shibata A et al. Inhibition of NF-kappaB activity decreases the VEGF mRNA expression in MDA-MB-231 breast cancer cells. *Breast Cancer Res Treat.* 2002;73(3):237–243.

215. Kiriakidis S et al. VEGF expression in human macrophages is NF-kappaB-dependent: studies using adenoviruses expressing the endogenous NF-kappaB inhibitor IkappaBalpha and a kinase-defective form of the IkappaB kinase 2. *J Cell Sci.* 2003;116(Pt 4):665–674.

216. Torisu H et al. Macrophage infiltration correlates with tumor stage and angiogenesis in human malignant melanoma: Possible involvement of TNFalpha and IL-1alpha. *Int J Cancer.* 2000;85(2):182–188.

217. Salvesen HB, Akslen LA. Significance of tumour-associated macrophages, vascular endothelial growth factor and thrombospondin-1 expression for tumour angiogenesis and prognosis in endometrial carcinomas. *Int J Cancer.* 1999;84(5):538–543.

218. Takanami I, Takeuchi K, Kodaira S. Tumor-associated macrophage infiltration in pulmonary adenocarcinoma: Association with angiogenesis and poor prognosis. *Oncology.* 1999;57(2):138–142.

219. Lamagna C, Aurrand-Lions M, Imhof BA. Dual role of macrophages in tumor growth and angiogenesis. *J Leukoc Biol.* 2006;80(4):705–713.

220. Kono Y, Kawakami S, Higuchi Y, Yamashita F, Hashida M. In vitro evaluation of inhibitory effect of nuclear factor-kappaB activity by small interfering RNA on pro-tumor characteristics of M2-like macrophages. *Biol Pharm Bull.* 2014;37(1):137–144.

221. Wu H et al. Tumor-associated macrophages promote angiogenesis and lymphangiogenesis of gastric cancer. *J Surg Oncol.* 2012;106(4):462–468.

222. Seo KH et al. Essential role for platelet-activating factor-induced NF-kappaB activation in macrophage-derived angiogenesis. *Eur J Immunol.* 2004;34(8):2129–2137.

223. Nozawa H, Chiu C, Hanahan D. Infiltrating neutrophils mediate the initial angiogenic switch in a mouse model of multistage carcinogenesis. *Proc Natl Acad Sci USA.* 2006;103(33):12493–12498.

224. Shang K et al. Crucial involvement of tumor-associated neutrophils in the regulation of chronic colitis-associated carcinogenesis in mice. *PLoS One.* 2012;7(12):e51848.

225. Kuang D-M et al. Peritumoral neutrophils link inflammatory response to disease progression by fostering angiogenesis in hepatocellular carcinoma. *J Hepatol.* 2011;54(5):948–955.

226. Martinon F, Burns K, Tschopp J. The inflammasome: a molecular platform triggering activation of inflammatory caspases and processing of proIL-beta. *Mol Cell.* 2002;10(2):417–426.

227. Cook GP, Savic S, Wittmann M, McDermott MF. The NLRP3 inflammasome, a target for therapy in diverse disease states. *Eur J Immunol.* 2010;40(3):631–634.

228. Kong H et al. Differential expression of inflammasomes in lung cancer cell lines and tissues. *Tumour Biol.* 2015;36(10):7501–7513.

229. Zitvogel L, Kepp O, Galluzzi L, Kroemer G. Inflammasomes in carcinogenesis and anticancer immune responses. *Nat Immunol.* 2012;13(4):343–351.

230. Fabbi M, Carbotti G, Ferrini S. Context-dependent role of IL-18 in cancer biology and counter-regulation by IL-18BP. *J Leukoc Biol.* 2015;97(4):665–675.

231. Apte RN, Voronov E. Is interleukin-1 a good or bad "guy" in tumor immunobiology and immunotherapy?. *Immunol Rev.* 2008;222:222–241.

232. Liu K, Abrams SI. Coordinate regulation of IFN consensus sequence-binding protein and caspase-1 in the sensitization of human colon carcinoma cells to Fas-mediated apoptosis by IFN-gamma. *J Immunol.* 2003;170(12):6329–6337.

233. Kim HS et al. Systematic identification of molecular subtype-selective vulnerabilities in non-small-cell lung cancer. *Cell.* 2013;155(3):552–566.

234. Sorrentino R et al. Human lung cancer-derived immunosuppressive plasmacytoid dendritic cells release IL-1α in an AIM2 inflammasome-dependent manner. *Am J Pathol.* 2015;185(11):3115–3124.

235. Machida EO et al. Hypermethylation of ASC/TMS1 is a sputum marker for late-stage lung cancer. *Cancer Res.* 2006;66(12):6210–6218.

236. Stehlik C et al. The PAAD/PYRIN-family protein ASC is a dual regulator of a conserved step in nuclear factor kappaB activation pathways. *J Exp Med.* 2002;196(12):1605–1615.

237. El Rayes T et al. Lung inflammation promotes metastasis through neutrophil protease-mediated degradation of Tsp-1. *Proc Natl Acad Sci USA.* 2015;112(52):16000–16005.

238. Brandt E, Van Damme J, Flad HD. Neutrophils can generate their activator neutrophil-activating peptide 2 by proteolytic cleavage of platelet-derived connective tissue-activating peptide III. *Cytokine.* 1991;3(4):311–321.

239. Cohen AB, Stevens MD, Miller EJ, Atkinson MA, Mullenbach G. Generation of the neutrophil-activating peptide-2 by cathepsin G and cathepsin G-treated human platelets. *Am J Physiol.* 1992;263(2 Pt 1):L249–L256.

240. Nufer O, Corbett M, Walz A. Amino-terminal processing of chemokine ENA-78 regulates biological activity. *Biochemistry.* 1999;38(2):636–642.

241. Wilson TJ, Nannuru KC, Futakuchi M, Singh RK. Cathepsin G-mediated enhanced TGF-beta signaling promotes angiogenesis via upregulation of VEGF and MCP-1. *Cancer Lett.* 2010;288(2):162–169.